

Research article

Geology and engineering properties of sensitive Boston Blue Clay at Newbury, Massachusetts

Don J. DeGroot^{1,*}, Melissa E. Landon² and Steven E. Poirier³

¹ Department of Civil and Environmental Engineering, University of Massachusetts Amherst, Amherst, MA, 01003 USA

² Department of Civil and Environmental Engineering, University of Maine, Orono, ME, 04469 USA

³ Geosyntec Consultants, Acton, MA, 01720 USA

* **Correspondence:** Email: degroot@umass.edu; Tel: +14135450088.

Abstract: This paper describes the geology and geotechnical engineering properties of a sensitive marine clay deposit at a research site located in Newbury, Massachusetts (MA) in the northeast USA. Results from in situ testing, soil sampling, and laboratory testing are presented. The clay is locally known as Boston Blue Clay (BBC) which is a glacial marine clay that was deposited approximately 14,000 years ago in the greater Boston, MA area during retreat of the Laurentide Ice Sheet. The thickness, stress history, and soil properties of BBC can vary significantly depending on location. At the Newbury research site, the BBC deposit consists of a shallow thin desiccated crust underlain by a 12-meter thick low plasticity clay with an overconsolidation ratio ranging from 2 to 3. Sensitivity of the clay ranges from approximately 10 to 30, based on field vane and fall cone measurements. In situ testing performed at the site included seismic piezocone and field vane. Soil sampling was performed using a variety of samplers including Sherbrooke block, fixed piston thin-walled Shelby tube, and a thick-walled drive sampler. A full suite of advanced laboratory tests was performed on the various quality samples collected, which ranged from very poor (thick-walled drive sampler) to excellent (Sherbrooke block), including constant rate of strain consolidation, consolidated undrained triaxial and direct simple shear. The efficacy of the Recompression and SHANSEP procedures to mitigate sample disturbance was evaluated using results from the advanced laboratory test program. The paper presents data from these advanced tests as well as other soil classification, index, and engineering properties based on in situ measurements and laboratory test results. A synopsis of constructed facilities built on and in BBC within the greater Boston area is also presented.

Keywords: soft clay; in situ testing; soil sampling; shear strength; consolidation

1. Introduction

This paper describes the geologic and geotechnical engineering properties of a sensitive glacial marine clay deposit at a research site in Newbury, Massachusetts (MA), northeast United States (U.S.), 60 km north of the City of Boston, MA (Figure 1). This deposit is widely found in eastern MA, the greater Boston region, and southern New Hampshire, is locally known as Boston Blue Clay (BBC), and has a thickness that can vary from a few meters up to 60 meters. BBC has undergone extensive desiccation due to freezing, ground water table fluctuations, possible erosion, and anthropogenic activities. As a result, the deposit often has a stiff overconsolidated crust below which is soft, low overconsolidation BBC. Significant variations in thickness of the crust and the overall deposit are due to the complex depositional environment and subsequent geologic history in the region. At the Newbury site, the deposit is approximately 12 m thick with a 2 m upper crust. The site was initially developed by the University of Massachusetts (UMass) Lowell for a research program on behavior of deep pile foundations. An extensive site investigation was conducted by Paikowsky and Chen [1] to determine representative geotechnical engineering properties for the pile research.

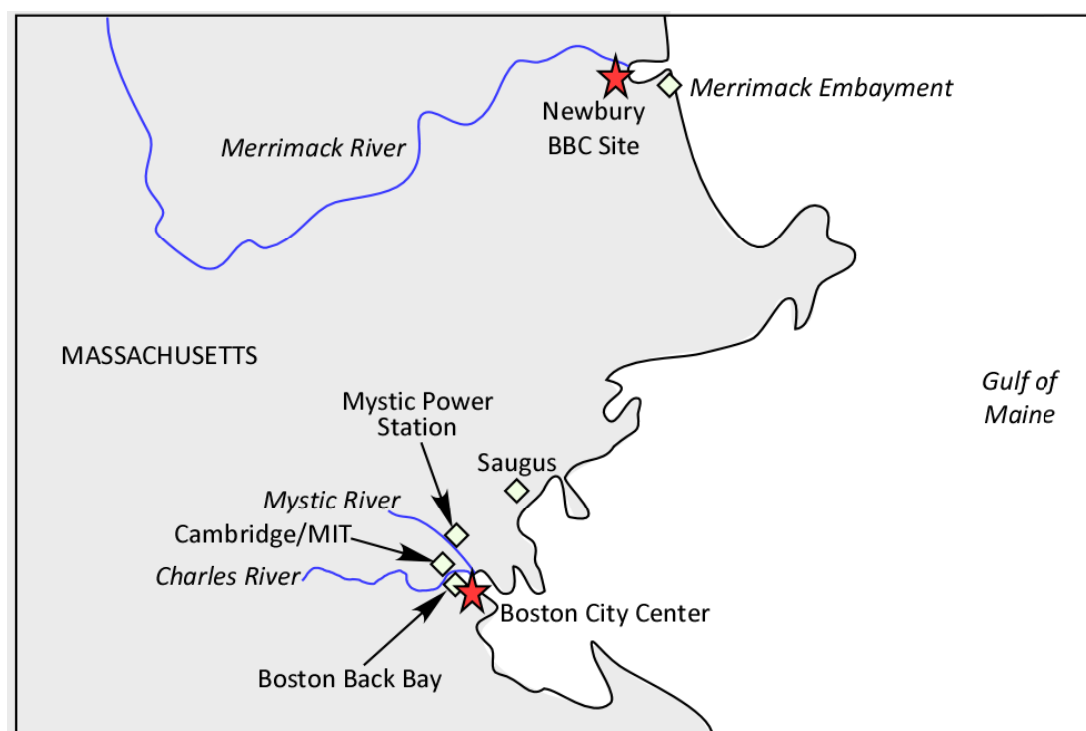


Figure 1. Location map showing Newbury, MA BBC test site and other referenced locations.

In 2000, UMass Amherst initiated a research program at the Newbury site with a primary focus on collection of high quality Sherbrooke block samples. The samples were collected to a depth of 10 m and a suite of classification and advanced laboratory tests were conducted on the samples. Other sampling methods were also deployed at the site to study non-destructive methods of assessing

sample quality and the impact of sample quality on measured soil behavior and selection of engineering design parameters. Table 1 lists some of in situ tests, soil sampling, and laboratory tests conducted at the site by UMass Amherst together with a listing of measured variables, interpreted parameters, and basic test methods followed. Representative data from most of these tests are presented in this paper which synthesizes the work of several UMass Amherst dissertations [2–5]. The paper describes the geology of the greater Boston area and some example geotechnical profiles. Results from the in situ and laboratory tests are presented and evaluated. Comparisons are made with published data for natural BBC and the paper concludes with a discussion of engineering problems encountered with BBC.

2. Engineering geology

2.1. Glaciation

The Gulf of Maine, which extends from Cape Cod to southern Nova Scotia, was glaciated during the Wisconsin glacial period as recently as 12 to 17 thousand calendar years before present (ka) [6–9]. Kenney [9] and Barosh and Woodhouse [10] indicate that glacial activity in the Boston region scoured the bedrock, creating a highly variable, undulating surface with ridges oriented predominantly in the north-south direction. Figure 2 illustrates this undulating bedrock surface for the Merrimack River Embayment within which the Newbury site is located. In some areas, glacial deposits were not entirely scoured away, and glacial till is routinely found below the subsequently deposited glaciomarine sediments, which includes BBC.

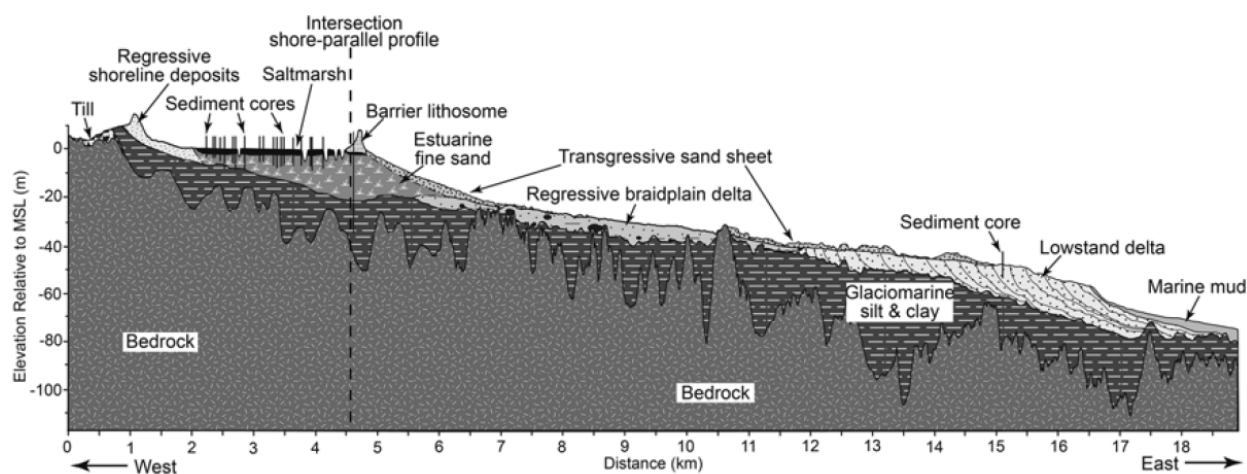


Figure 2. Merrimack River Embayment shore-normal cross-section [6].

2.2. Depositional environment

In periglacial environment, relative sea level (RSL) variations were dependent on the rate of glacial retreat and isostatic rebound of the crust in the area. Prior to glacial retreat, the marine limit occurred around 16 to 17 ka where RSL was 31 to 33 m above modern mean sea level (MSL) [17]. Schnitker et al. [18] indicate that the entire Gulf of Maine was ice free around 14 ka, and show that

the Boston Basin and Merrimack Embayment locations were both just at the margin of the glacier at this time. Ridge et al. [19] demonstrates evidence of northern glacier retreat along the northern Massachusetts, New Hampshire, and southern Maine coasts progressively occurring from 13 to 14 ka.

Table 1. Summary of in situ tests, soil sampling, and laboratory tests for the Newbury, BBC site.

| Test | Measurements | Interpreted Properties | Methods/Comments |
|--|-------------------------------|---|--|
| In Situ | | | |
| Standard Penetration Test (SPT) | N | N_{60} | ASTM D1586 [11] |
| Field Vane Test (FV) | Torque | s_u, s_{ur} | ASTM D2573 [11] |
| Seismic Cone Penetration Test (SCPTU) | q_c, f_s, u, V_{vh} | σ'_p, s_u, G_{max} | ASTM D5778 [11]— u_2 cone, seismic |
| Equilibrium Pore pressure | u_0 | h_t | Open standpipe piezometers |
| Sampling | | | |
| Split spoon sampler (SS) | | | ASTM D1586 [11] |
| 76 mm (3") free (FP), fixed piston (MFP) | | | ASTM D1587 [11] |
| Sherbrooke Block | | | Lefebvre & Poulin [12], DeGroot et al. [13] |
| Laboratory | | | |
| Water content | w | | ASTM D2216 [11] |
| Specific Gravity | G_s | | ASTM D854 [11] |
| Atterberg Limits | w_L, w_p | I_p, I_L | ASTM D4318 [11] |
| Grain Size Distribution | | % sand, silt, clay | ASTM D422 [11] |
| Unit Weight | γ_b, γ_d | | |
| Carbonate Content | % Carbonates | | Driemanis [14] |
| SEM | sample image | | JEOL JSM-5400 Scanning Microscope |
| Cation Exchange Capacity | CEC | | 1 N neutral Ammonium Acetate Extraction Method |
| Organics | % organics | | ASTM 2974 [11] |
| Pore water chemistry | cations/anions | | Ion Chromatography EPA-300, ASTM D5847 [11] |
| Sample suction and shear wave velocity | $u_s, V_{vh}, V_{hh}, V_{hv}$ | σ'_s | Landon et al. [15], Poirier et al. [16] |
| Strength index: Torvane, fall cone (intact and remolded) | | s_u, s_{ur} | |
| IL consolidation | $\sigma'_{v-\varepsilon-t}$ | $\sigma'_p, C_{re}, C_{ce}, c_v, c_\alpha, k_v$ | ASTM D2435 [11] |
| CRS Consolidation | $\sigma'_{v-\varepsilon-t}$ | $\sigma'_p, C_{re}, C_{ce}, c_v, k_v$ | ASTM D4186 [11] |
| Triaxial: UUC, CAUC, CK_0UC | ε, q, p, u | c', ϕ', s_u, s_d, E | ASTM D4767 [11], D2850 [11], Recompression and SHANSEP |
| Direct Simple Shear | $\gamma, \tau_h, \sigma'_v$ | s_u, G | Geonor DSS, ASTM D6528 [11], Recompression and SHANSEP |

Glaciomarine sediment deposition in the region was initiated during glacial period of the late Pleistocene, around 17.5 to 15.5 ka, and accelerated in the periglacial period [6]. Kenney [9] indicates the glaciomarine sediment was deposited between 13.5 and 14.5 ka in the Boston Basin. Kaye [20] provides further evidence that this material was deposited in the cold periglacial environment based on the presence of cold weather pollen and embedded cobbles and small stones common for ice rafting. Kaye [20], however indicates an older timeline around 26 to 28 ka for deposition and 15 to 26 ka for oxidation during low sea level of the glaciomarine sediment, likely the result of limitations to radioisotope dating at the time. Kaye [21] and Mesri and Ali [22]—conclude that low concentrations of foraminifera in the BBC suggests deposition in a salt water environment, however, the absence of abundant marine shells suggests this environment was of low salinity.

2.3. Deposition and source material

The material that formed the glaciomarine sediment was eroded bedrock and glacial deposits (i.e., till) from glacial activity and transported by meltwater before settling out in the marine environment [6]. The glaciomarine sediment drapes over the undulating bedrock surface and consists of silty clay with some sand and gravel layers and is progressively more sandy in the upper portion of the deposit [6,9,23]. This glaciomarine deposit is typically referred to as Boston Blue Clay in Massachusetts and Presumpscot Formation in New Hampshire and Maine.

In the Merrimack Embayment, the upper surface of the glaciomarine is located around –15 to –20 m MSL in the area bounded by the modern shoreline and the Merrimack and Parker Rivers [6]. The deposit is buried beneath subsequently deposited sandy materials, which will be discussed in Section 2.4. In the Boston Basin, the maximum elevation that glaciomarine clay was deposited is 15 m MSL [9]. The thickness of the glaciomarine sediment is estimated to be generally between 12 m and 43 m in the Boston Basin and can reach up to 60 m in the western portion of the area [9,23]. The thickness of the glaciomarine sediment can be in excess of 20 m in the Merrimack Embayment [6].

2.4. Post depositional processes

The marine low stand occurred around 12 to 14 ka, where RSL was around –41 to –45 m MSL [6,7,24] as a result of isostatic rebound of Earth's crust following glacial retreat. During this time, the glaciomarine clay in some locations would have been exposed to erosion. Several sources identify an eroded, oxidized, desiccated, and overconsolidated clay crust at the top of the glaciomarine sediment [6,9,20,23]. Glaciomarine sediment in the Boston Basin is overconsolidated to depths as great as 10 m [9] and 21 m [20] below the top of the deposit caused by post-depositional processes associated with isostatic uplift and subsequent erosion and desiccation prior to resumed deposition. Below this zone, the sediment is lightly overconsolidated to normally consolidated as erosion and deposition became balanced. Additionally, erosion channels have been identified in the glaciomarine sediment of the Boston Basin, which were subsequently infilled by coarse grained deposits [9].

Kenney [9], Hein et al. [6], and Johnson [20] discuss the complex sediment formations deposited atop the glaciomarine sediment and approximate timelines. Figures 3a,b shows profiles of typical geologic units identified from subsurface borings in the Boston Basin. Figures 2 and 4 provide general profiles for the Merrimack Embayment, and Figure 3c shows the geologic units for

the Newbury site. The glaciomarine sediment is overlain by fine to coarse sand and silt outwash deposits in the Boston Basin and fine sand and silt paleodeltas in the Merrimack Embayment deposited during RSL low stand. Following these deposits and subsequent sea level rise, estuarine salt marshes and highly organic silt and fine sand sediments were deposited. Lastly, the greater Boston area has a long history of anthropomorphic activities and land building to maximize useable space for population and industry growth, and much of the ground near the surface consists of miscellaneous fills consisting of rubble, wood, sand and gravels.

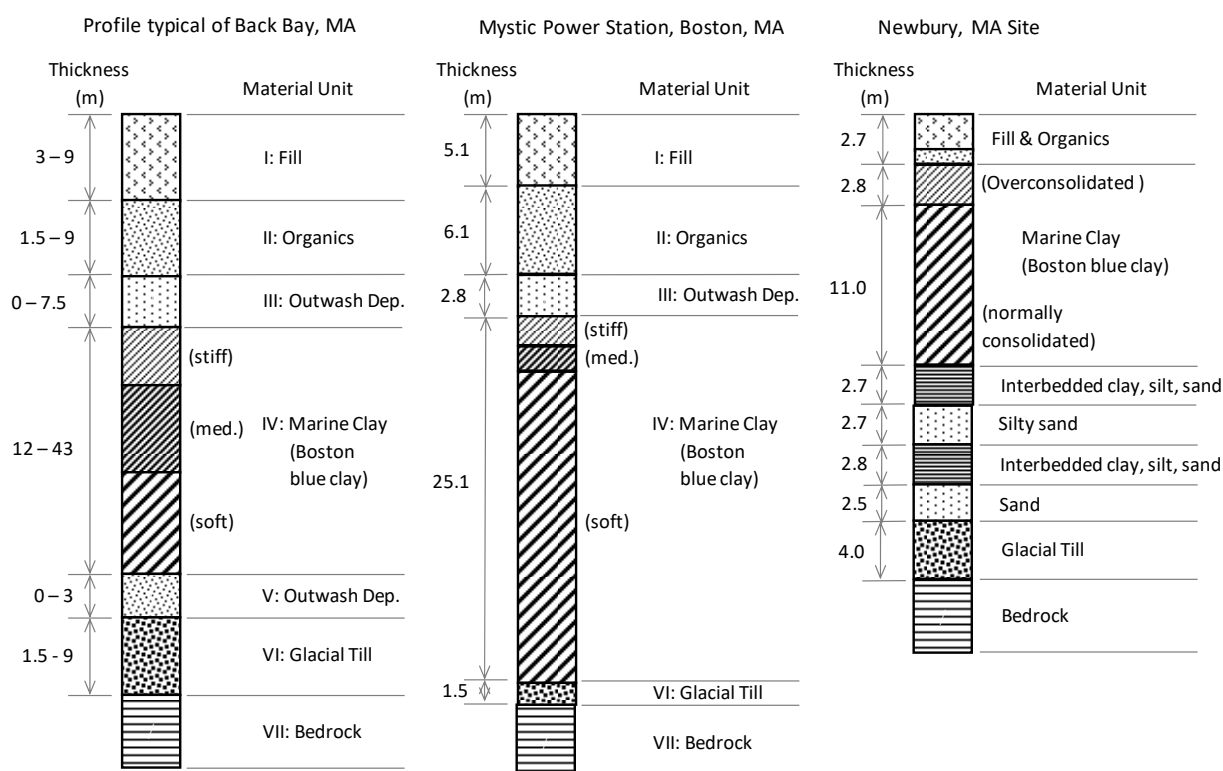


Figure 3. Subsurface profiles illustrating geologic units (after [23]) found in: a) a site in Back Bay, Boston, MA [23], b) the site of the now Mystic Generating Station in Boston, MA [9], and c) the Newbury, MA site [25].

3. Soil composition

Grain size data from hydrometer analyses for the Newbury BBC soft clay gives approximately 60% clay size fraction ($CF = \% < 0.002$ mm), 40% silt fraction (% between 0.002 mm and 0.075 mm), and trace sand (Table 2, Figure 5). X-Ray diffraction results indicate the mineralogy of the soft clay consists predominantly of chlorite, illite, quartz, and feldspar. Chemical testing of the soil consisted of: pH measurement on a 1:1 mix of soil and distilled water; % organic matter using a muffle furnace; cation exchange capacity (CEC) measured using a 1 N neutral ammonium acetate extraction method; and total carbonates using a Chittick apparatus [14]. Results (Table 3) show the soft clay is slightly basic and with low values of organic content ($< 1\%$), cation exchange capacity (< 10 meq/100 g), and carbonate content ($\approx 8\%$). Results of tests on pore fluid extracted from samples conducted using a high pressure liquid chromatography apparatus (Table 3) show sodium

and chloride ions dominate, however at concentrations well below that of seawater. This is consistent with a low salinity depositional environment discussed in Section 2.2.

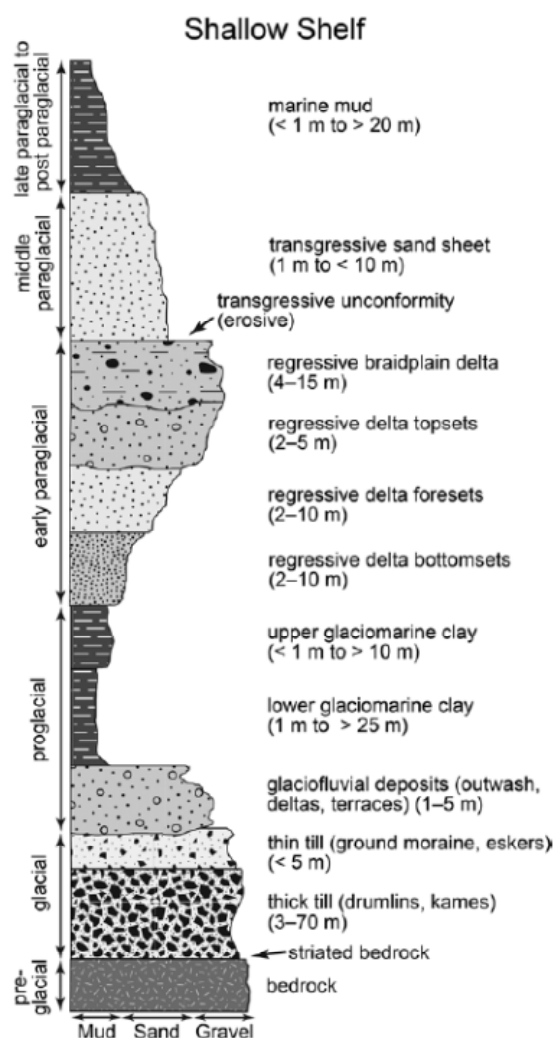


Figure 4. Representative geologic stratigraphic units along a shallow-shelf “palaeodelta sequence offshore a river-associated paraglacial barrier” like that of the Merrimack River Embayment in Massachusetts [6].

Table 2. Typical average Newbury BBC classification and index properties.

| Soil Unit | Sand (%) | Silt (%) | Clay (%) | Density ρ_t (kg/m ³) | Solids ρ_s (kg/m ³) | w (%) | w _L (%) | w _P (%) | I _p (%) | I _L (-) | A (-) |
|-----------------------------|----------|----------|----------|---------------------------------------|--------------------------------------|-------|--------------------|--------------------|--------------------|--------------------|-------|
| Crust ≈ 3 to 5 | 9 | 37 | 54 | 1840 | 2760 | 40 | 48 | 29 | 19 | 0.58 | 0.36 |
| Upper soft clay ≈ 5 to 6 | 1 | 36 | 63 | 1810 | 2780 | 43 | 47 | 26 | 21 | 0.81 | 0.33 |
| Soft clay ≈ 6 to 10+ | 1 | 38 | 62 | 1740 | 2770 | 50 | 47 | 28 | 19 | 1.16 | 0.32 |

Table 3. Typical organic and chemical properties of Newbury BBC.

| Soil Unit Depth (m) | pH | OC (%) | CEC (meq/g) | TC (%) | SS (dS/m) | Na ⁺ (mg/L) | K ⁺ (mg/L) | Ca ⁺² (mg/L) | Mg ⁺² (mg/L) | Cl ⁻ (mg/L) | SO ₄ ⁻² (mg/L) |
|-----------------------------|-----|-----------|----------------|-----------|--------------|---------------------------|--------------------------|----------------------------|----------------------------|---------------------------|---|
| Crust ≈ 3 to 5 | 8.2 | 0.9 | 0.09 | 8.1 | 0.24 | 258 | 5 | 18 | 20 | 250 | 41 |
| Upper soft clay ≈ 5 to 6 | 8.1 | 0.7 | 0.09 | 7.5 | 0.54 | 265 | 8 | 16 | 14 | 255 | 65 |
| Soft clay ≈ 6 to 10+ | 8.4 | 0.8 | 0.08 | 8.1 | 0.51 | 280 | 9 | 15 | 10 | 260 | 76 |

OC = organic content, CEC = cation exchange capacity, TC = Total carbonates, SS = soluble salts.

4. In Situ State, index properties and structure

Open standpipe piezometer measurements indicate the in situ pore water pressure is hydrostatic, where the ground water table has an annual mean depth of 1.72 meters below ground surface. Natural water content (w) and void ratio (e) for the Newbury BBC is lowest in the shallow crust due to desiccation and possible erosion. Water content values are around the liquid limit (w_L) and fairly constant with depth within the soft clay. Likewise, total density is highest in the crust ($\rho_t \approx 1840 \text{ kg/m}^3$) and lowest in the soft clay ($\rho_t \approx 1740 \text{ kg/m}^3$). The density of solids is uniform throughout the deposit, with ρ_s averaging 2770 kg/m^3 . Table 2, Figure 5, and Figure 6 summarize Atterberg Limits data. The results plot around the A-line in the Plasticity chart, giving Unified Soil Classification System (USCS) classifications of ML (low plasticity silt) or CL (low plasticity clay). Atterberg limits are consistent with depth, with an average liquid limit (w_L) of 47, plastic limit (w_P) of 27, and plasticity index (I_P) of 20. The corresponding liquidity index ($I_L = (w - w_P)/I_P$) is well below one within the crust and is slightly greater than one within the soft clay. Activity values (I_P/CF) of approximately 0.33 are low compared to that of pure illite ($A = 0.90$) and chlorite clay minerals [26]. The low values indicate a portion of the measured clay fraction could be pulverized rock flour, which would not contribute to Activity.

Figure 7 plots the in situ void index ($I_{v0} = (e_0 - e^*_{100})/C^*_c$) versus σ'_{v0} for the deposit over the depth range from which block samples were collected. The I_{v0} data were computed using data from an incremental load (IL) consolidation test performed on a specimen of Newbury BBC remolded to approximately 1.25 times the liquid limit water content. The results give an intrinsic void ratio $e^*_{100} = 0.841$ at vertical effective stress $\sigma'_v = 100 \text{ kPa}$ and a slope of the remolded $e\text{-log}\sigma'_v$ compression curve between 100 and 1000 kPa, $C^*_c = 0.217$. Also plotted in Figure 7 are the Intrinsic Compression Line (ICL) and Sedimentation Compression Line (SCL) from Burland [27] and $I_{v0}\text{-}\sigma'_{v0}$ values from CRS and IL specimens. Specimen $I_{v0}\text{-}\sigma'_{v0}$ values show marked differences relative to the ICL and SCL lines. The shallower crust $I_{v0}\text{-}\sigma'_{v0}$ values plot just below the ICL, which is indicative of stiff, overconsolidated clay, whereas the deeper, soft clay specimen $I_{v0}\text{-}\sigma'_{v0}$ values plot well above the SCL, which suggests a soil with some sensitivity and possible cementation bonding [27,28]. The transition from crust to the soft clay is quite abrupt within the approximately 4 to 5 meter depth interval. Also plotted are compression curves from constant rate of strain (CRS) consolidation tests conducted on Sherbrook block samples (described subsequently in Section 6.0) collected from within

the crust (depth $z = 4.3$ m), the upper soft clay unit ($z = 5.6$ m) and the deeper soft clay unit ($z = 6.4$ m). The deeper soft clay shows significant destructuring for loading beyond the preconsolidation or yield stress, whereas the crust shows markedly different behavior with rounded compression and no clear yield stress, as is characteristic for stiff, desiccated clays. All three compression curves indicate a convergence at large strains to the SCL, but not the ICL. This indicates that even though significant destructuring has taken place for all specimens and especially the deeper soft clay unit specimen, some structure remains in the clay at large strains. According to Nagaraj and Miura [29], non-convergence of the curves with that for remolded specimens (i.e., the ICL in Figure 7) is an indication of the persistence of cementation of soil particles even after significant destructuring.

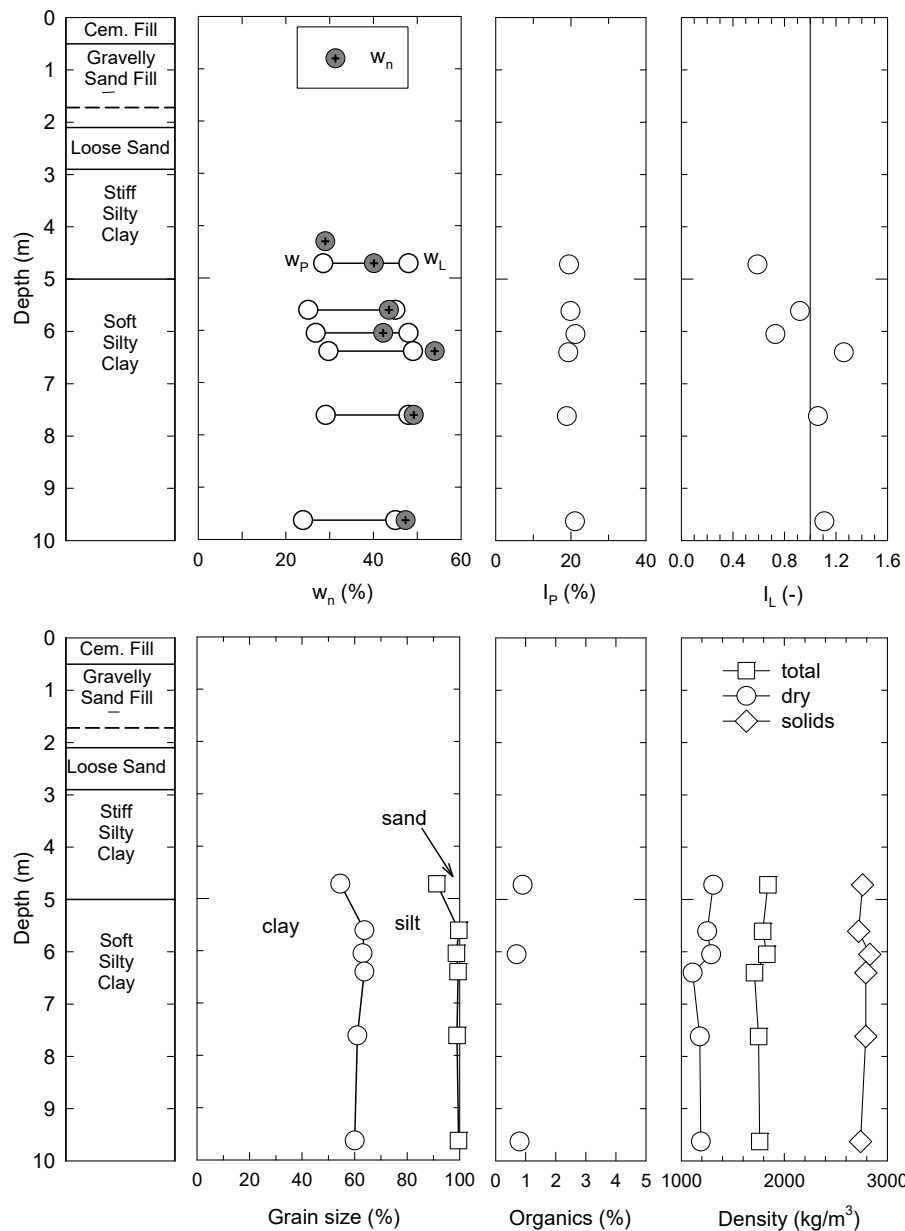


Figure 5. Newbury, MA site soil profile and depth plots of water content, Atterberg Limits, liquidity index, grain size, organic content and densities (values in Tables 2 and 3).

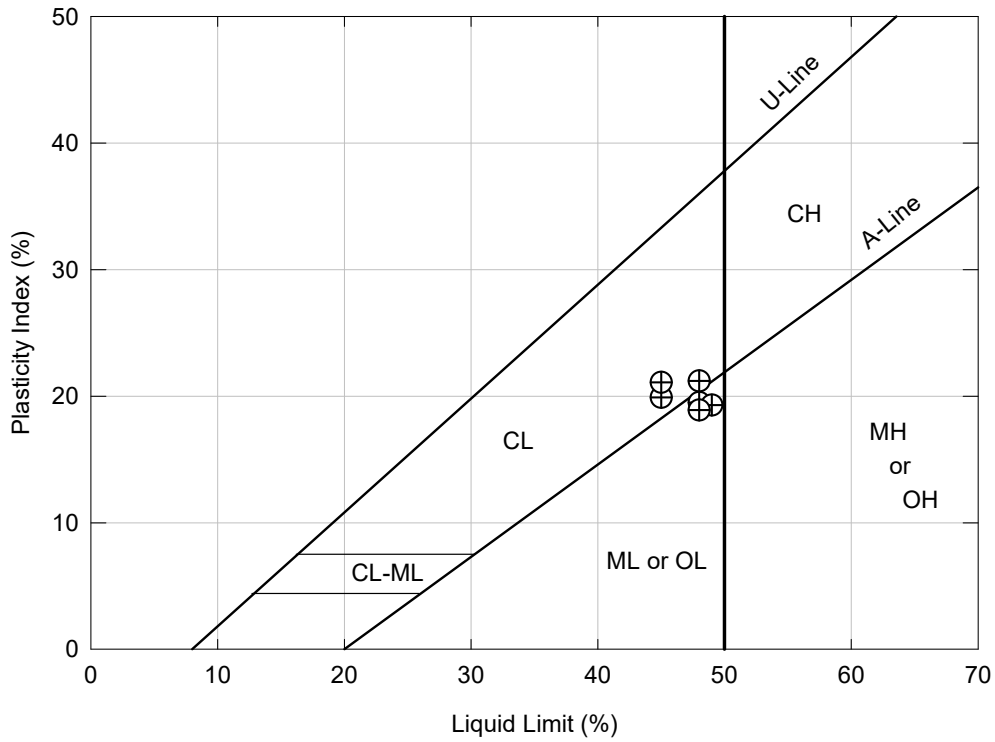


Figure 6. Plasticity Chart for Newbury BBC.

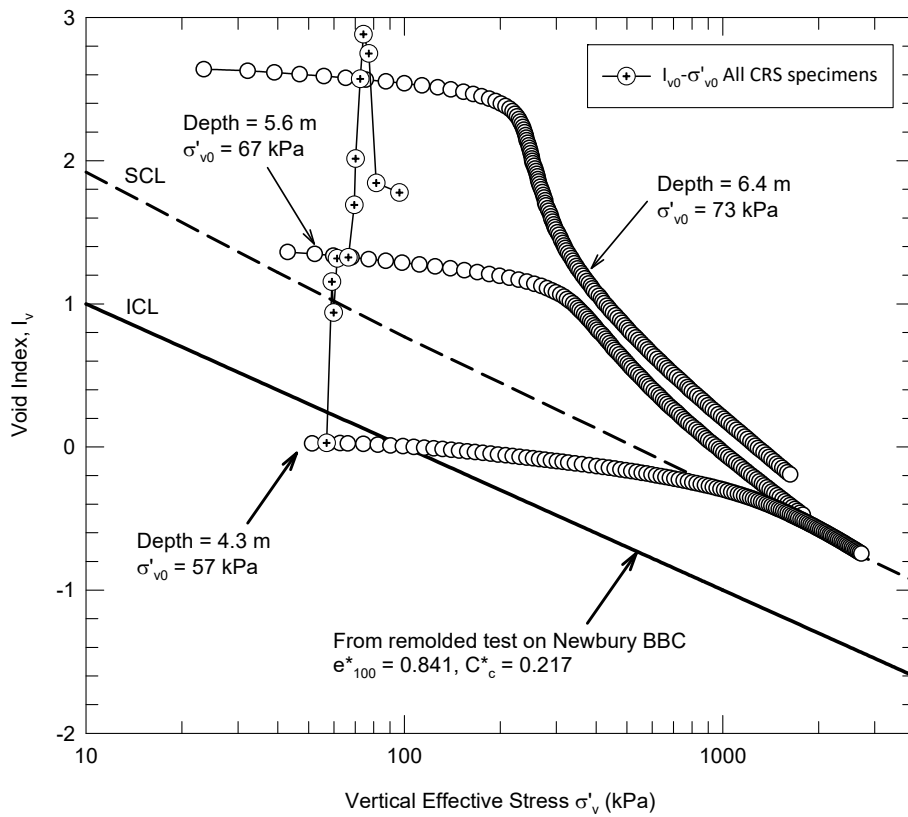


Figure 7. Newbury BBC in situ void index versus effective stress and CRS compression behavior.

Figure 8 illustrates pictorial evidence of an open flocculated structure within the soft clay unit. The scanning electron microscope (SEM) image was taken for a specimen prepared from a Sherbrooke block sample collected from 7.6 m depth. The SEM image was obtained using a JEOL JSM-5400 Scanning Microscope at 10 kV on an air dried specimen sputter coated with platinum.

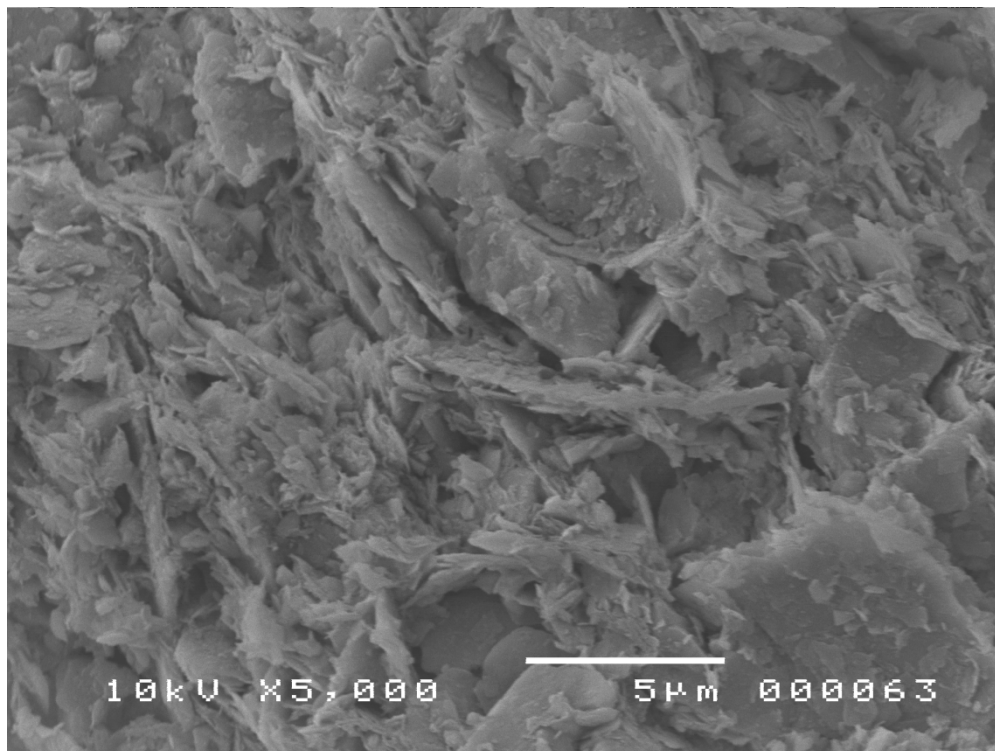


Figure 8. Scanning electron microscope image of Newbury BBC from a Sherbrooke block sample collected from depth of 7.6 m.

5. Engineering properties

Sherbrooke block samples were collected following the procedures of Lefebvre and Poulin [12] and DeGroot et al. [13] using a barite weighed drilling mud. Sample sealing, transport, and storage practices used are described in DeGroot et al. [13,30]. Additionally, several other tube sampling methods were performed at the site to study the influence of sampling procedures and tools on sample quality. All consolidation, triaxial, and direct simple shear specimens were extracted from the tube samples using the debonding procedure described in Ladd and DeGroot [31]. The baseline or reference stress-strain-strength behavior of the soil is considered that measured on the block sample specimens, and Section 5.5 compares these measured engineering properties to those obtained from specimens from other, typically less desirable, sampling methods.

Measured data from various in situ tests are first presented with little to no direct interpretation of engineering properties. Engineering properties based primarily on advanced laboratory tests conducted on high quality Sherbrooke block samples are then subsequently presented. Lastly, laboratory measurements are compared to in situ test data that give direct measures of engineering

properties (e.g. s_u from field vane) or in situ test data using correlations to predict engineering properties (e.g. N_{kt} for CPTU data based on laboratory s_u measurements).

5.1. In situ tests—measurements

Figure 9 plots measured data from a piezocone (CPTU) test conducted using a 10 cm² cone, 60° apex tip angle, with pore pressure measured behind the cone shoulder (u_2). The pore pressure system was saturated using silicone oil. The corrected tip resistance q_t was computed as $q_t = q_c + (1 - a) u_2$, where q_c = measured tip resistance and a = net area ratio (0.80 as per the manufacturer). The q_t , sleeve friction (f_s), and u_2 profiles all show the transition from the upper stiff crust into the softer clay below approximately 6 m. Between 6 m and 14 m, q_t values are less than one, indicative of a soft clay. At approximately 10 m depth and greater, decreasing u_2 values suggest decreasing clay content until around 14 m, where interbedded layers of clay, silt, and sand are encountered and u_2 occasionally drops to u_0 and below (Figure 9). Normalized cone resistance, $Q_t = (q_t - \sigma_{v0})/\sigma'_{v0}$, systematically decreases with depth below the crust until the interbedded units are reached. Values of the Robertson [32] soil behavior type (SBTn) index, I_c , for the main soft clay unit are within the range of 2.95 to 3.60, which corresponds to a soil behavior type of 'clays'. Figure 10 plots the data in Robertson [33] soil behavior type charts, where the crust, soft clay, and interbedded units are nominally separated. Below 14 m, the normalized pore pressure parameter, $B_q = (u_2 - u_0)/(q_t - \sigma_{v0})$, periodically drops down to zero and slightly less than zero, indicative of sand layers.

Shear wave velocity was measured using the seismic module on the piezocone (SCPTU) during the one meter rod breaks. Shear waves were generated at the ground surface using a steel channel beam equipped with a steel hammer on a pendulum. The beam was placed next to the cone rods and below an outrigger from the drill rig to provide normal stress. The raised hammer was allowed to free fall and strike a plate which generated a repeatable high amplitude shear wave with little to no compression wave. The resulting shear waves were vertically propagating and horizontally polarized (V_{vh}). Hammer strike and shear wave arrival at the cone were recorded with triaxial geophones. Shear wave velocity was interpreted using the pseudo-interval method [34] with both cross-correlation (CC) and cross-over (CO) methods [35]. The shear wave velocity (V_{vh}) profile plotted in Figure 11a show an initial decrease within the crust and thereafter a progressive increase with increasing depth. Representative V_{vh} values were used with laboratory measured total density values (Figure 5) to compute small strain shear modulus, $G_{vh} = \rho_t V_{vh}^2$, plotted in Figure 11b.

No in situ measurements were made for horizontal shear wave velocity (e.g., using crosshole geophysics). Landon and DeGroot [36], however, conducted shear wave velocity measurements on Sherbrooke block samples in the laboratory using a set of bender element platens and measured V_{vh} as well as V_{hv} and V_{hh} . Data from four block samples from within the soft clay unit were converted to shear modulus and yielded ratios of $G_{hv}/G_{vh} = 1.20$ and $G_{hh}/G_{vh} = 1.68$, which were near constant with depth. These shear modulus anisotropy values are similar to those reported for other clays (e.g., [37,38]).

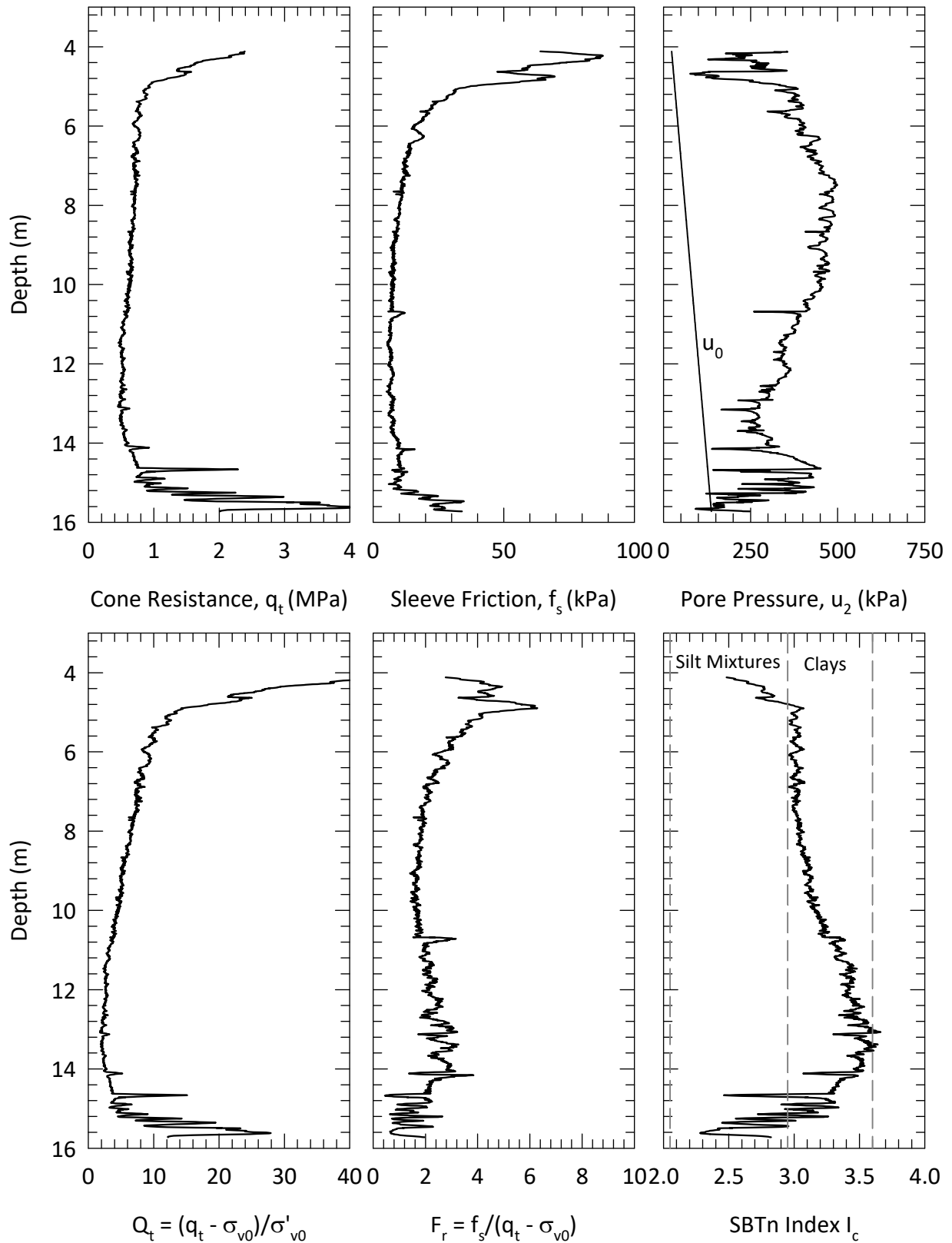
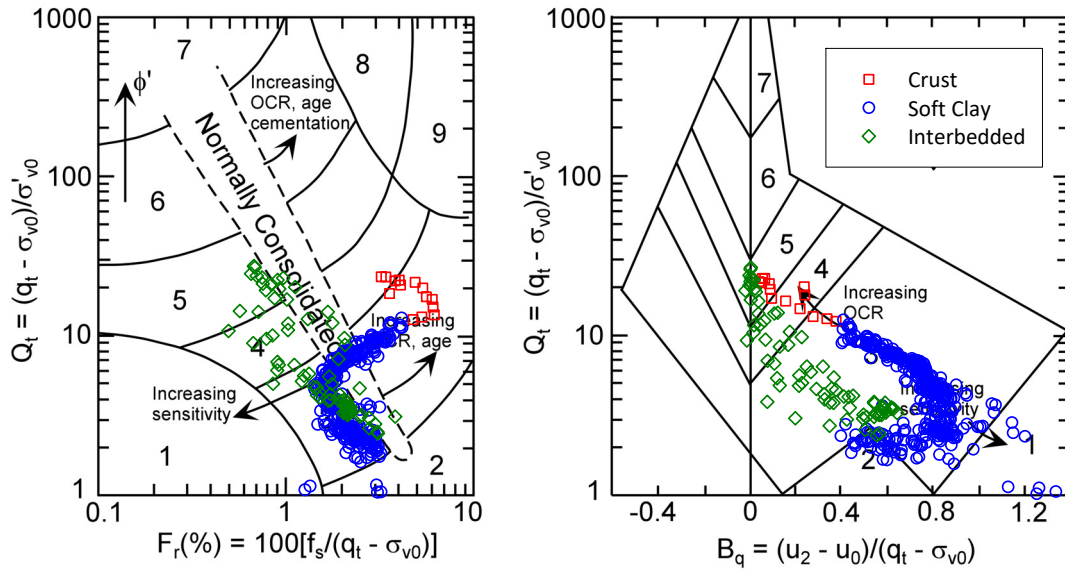


Figure 9. Newbury BBC CPTU profile.



Soil Behavior Type by Zone Number

- | | | |
|-----------------------------|--|-----------------------------------|
| 1. Sensitive, fine grained | 4. Silt mixtures clayey silt to silty clay | 7. Gravelly sand to sand |
| 2. Organic soils-peats | 5. Sand mixtures; silty sand to sand silty | 8. Very stiff sand to clayey sand |
| 3. Clays-clay to silty clay | 6. Sands; clean sands to silty sands | 9. Very stiff fine grained |

Figure 10. Newbury BBC CPTU data in Robertson [32] soil behavior type plots with nominal separation among the crust, soft clay, and interbedded clay, silt and sand units.

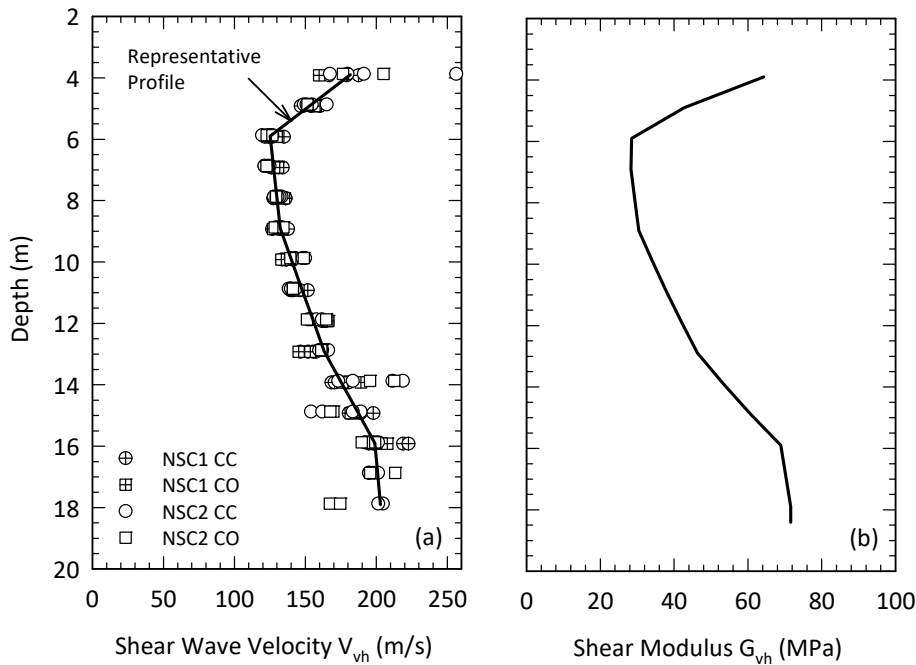


Figure 11. a) Newbury BBC shear wave velocity V_{vh} from two Seismic CPTU soundings using the CC = cross-correlation and CO = cross-over analysis methods, and b) interpreted shear modulus G_{vh} computed from representative V_{vh} profile.

Field vane (FV) shear tests were conducted using a Nilcon Vane Borer with a 130 mm × 65 mm vane and 1.9 mm thick rectangular blades (i.e., no taper) having a perimeter ratio of 4%. Rotation of the vane for all peak vane strength tests was conducted at 6°/min and initiated within 1 min of stopping the advance of the vane to a new test depth. Remolded vane strengths were determined at the same depth as the peak strength test after performing 10 rapid, full revolutions of the vane. Figure 12a plots the FV peak undrained shear strength (s_{uFV}) for three soundings and remolded undrained shear strengths ($s_{ur,FV}$) from one sounding. The s_{uFV} data show high, but scattered, values in the crust, followed by lower values averaging 20 kPa in the deeper soft clay unit that are essentially constant with depth. Sensitivity (s_u/s_{ur}) values within the deeper soft clay unit range from 8 to 38 with an average of about 15 (Figure 12b). The normalized undrained shear strength s_{uFV}/σ'_{v0} decreases rapidly with depth through the crust and thereafter at a slower rate in the main soft clay unit (Figure 12c).

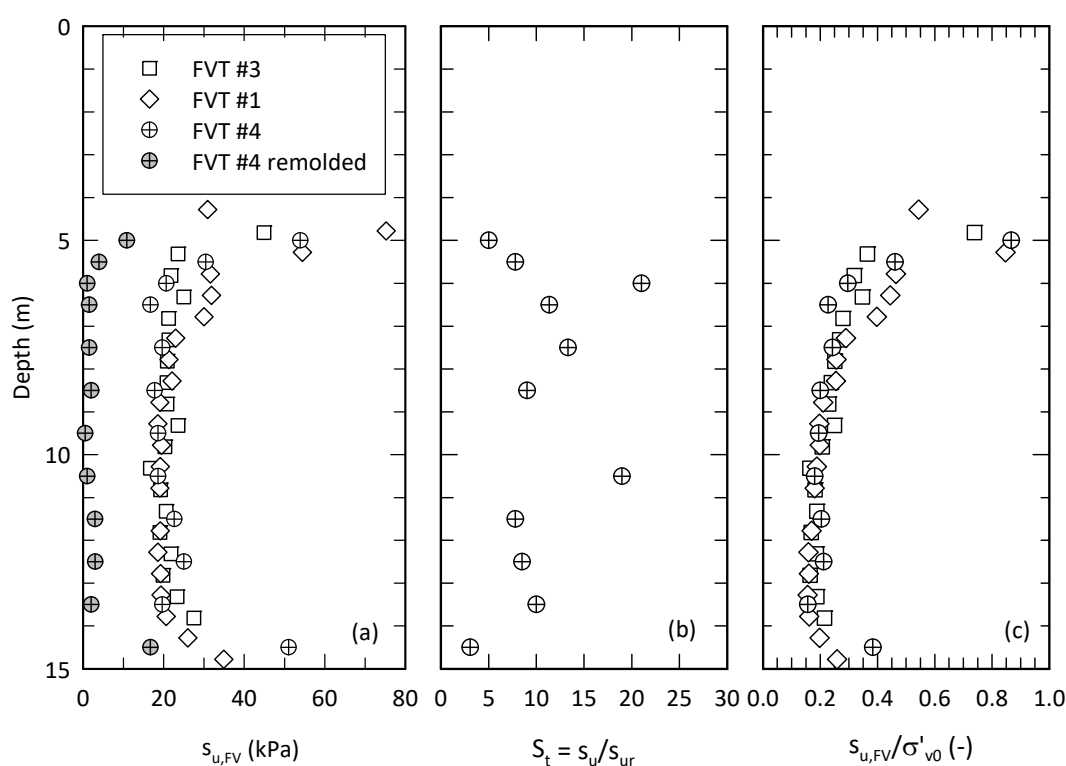


Figure 12. Newbury BBC field vane test a) peak and remolded undrained shear strength, b) sensitivity, and c) normalized undrained shear strength.

5.2. Stress history and compressibility

The stress history of BBC in the greater Boston area can vary significantly depending on site-specific geologic history as noted in Section 2. In most cases, however, the soil is overconsolidated at the top of the deposit primarily due to desiccation and possible erosion. At greater depths for locations that did not undergo significant erosion, the soil is lightly overconsolidated, most likely due to aging and physio-chemical bonding (e.g., cementation). Figure 13 plots typical compression curves from CRS consolidation tests on Sherbrooke block sample

specimens from three depths (the same shown in Figure 7). Results show significant changes in soil behavior over the 2 meter interval where the soil transitions from the crust to the soft clay unit. The curve for the specimen from within the crust ($z = 4.3$ m) is more rounded in ε - $\log\sigma'_v$ space. The specimen from within the soft clay unit ($z = 6.4$ m) has noticeably variable compressibility beyond the preconsolidation stress σ'_p (or yield stress, σ'_{vy}) that is characteristic of a structured soil. The compression ratio $C_{ce} = \Delta\varepsilon/\Delta\log\sigma'_v$ for $\sigma'_v > \sigma'_p$ is approximately constant at 0.14 for the 4.1 m deep specimen. However, the compression ratio for the 6.4 m specimen is maximum just beyond σ'_p , with $(C_{ce})_{max} = 0.75$, illustrating rapid destructuring, and decreases significantly to $(C_{ce})_{min} = 0.17$ when $\sigma'_v = 4 - 8\sigma'_p$.

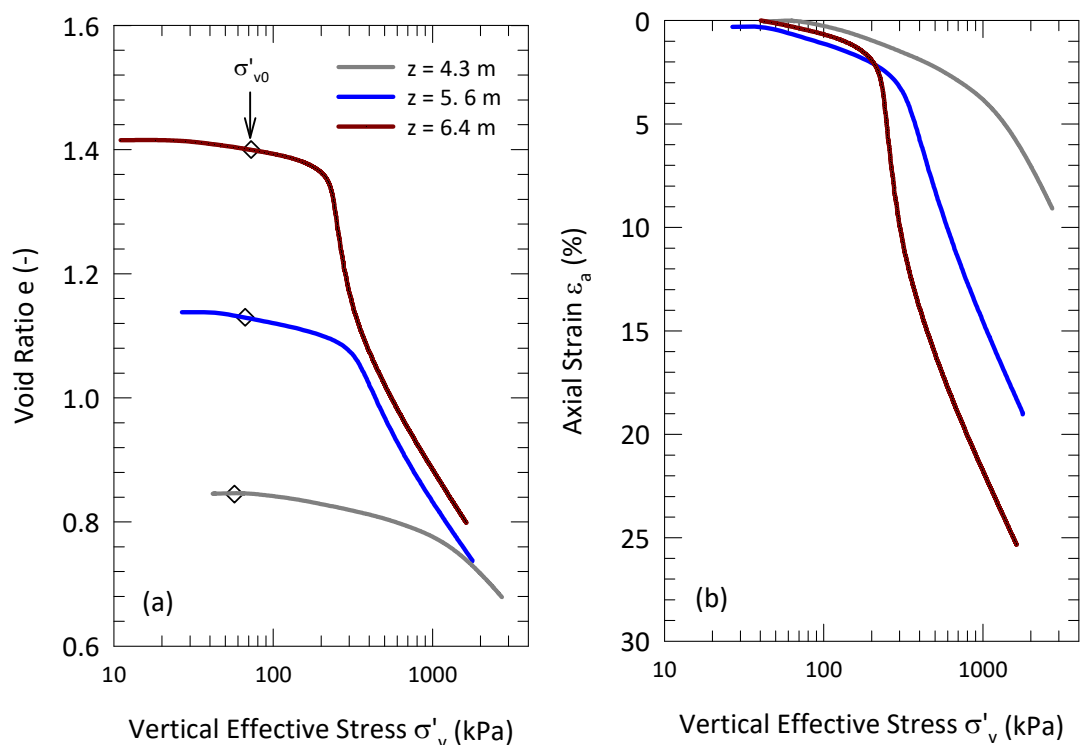


Figure 13. Newbury BBC one-dimensional CRS consolidation behavior: a) void ratio and b) axial strain.

Figures 14 and 15 highlight the advantage of conducting CRS tests for structured clays such as the soft clay at Newbury to ensure good resolution of the variation in behavior (compressibility and coefficient of consolidation) relative to σ'_p . The figures show data from both a CRS test and an incremental load (IL) oedometer test with 24 hr load increments and end of increment (EOI) strains. Even with a reduced load increment ratio ($LIR = [\sigma_{i+1} - \sigma_i]/\sigma_i$) of approximately 0.5 (Figure 14), end of primary σ'_p and $(C_{ce})_{max}$ would be incorrectly estimated for IL tests. The load increment close to σ'_p undergoes significant secondary compression consistent with the sharp increase in C_{ce} near σ'_p (i.e., because $C_{\alpha\varepsilon}/C_{ce}$ is a constant). The height-time curve does not have an inflection (Figure 15b), making it impossible to estimate end of primary consolidation using either the Taylor or Casagrande construction methods. For this reason, Ladd and DeGroot [31] suggest that if IL tests are conducted, all load increments should be interpreted for the equivalent end of primary consolidation (t_{100}) using

a constant time t_c equal to a representative value of t_{100} from the normally consolidated increments. Figure 15a shows an example for Newbury BBC, where interpreting load increments using t_c results in an estimate of the end of primary σ'_p that is much closer to that from the CRS test.

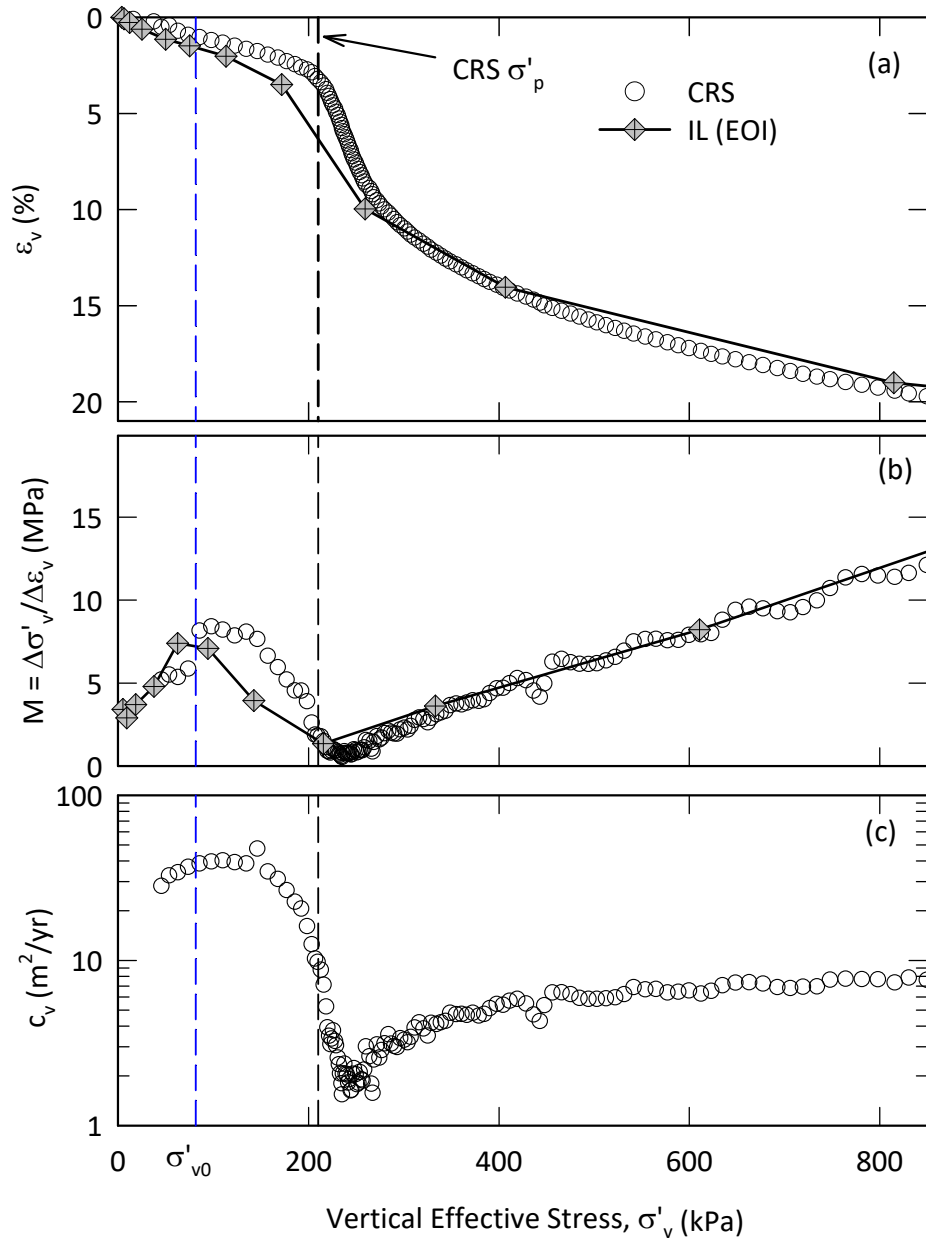


Figure 14. 1D CRS and IL consolidation test comparison conducted on Newbury BBC block samples from depth interval 7.3 to 7.6 m: a) compression, b) constrained modulus, and c) coefficient of vertical consolidation (modified from [39]).

Figure 16a plots stress history data from the full set of CRS tests conducted on Sherbrooke block sample specimens. Sample quality was assessed using the $\Delta e/e_0$ at σ'_{v0} method [40] and ε_a at σ'_{v0} Sample Quality Designation (SQD) method [41]. Values of $\Delta e/e_0$ at σ'_{v0} were less than 0.03, rating the samples as "very good to excellent", except the deepest specimen (9.8 m) has a $\Delta e/e_0$ at

σ'_{v0} value of 0.034, just outside this rating. Similarly, all values of ε_a at σ'_{v0} were less than 1.3%, rating all specimens as quality A or B. Sample qualities are discussed in more detail in Section 5.5, which compares them with those obtained from tube sample specimens.

All CRS tests were conducted at a strain rate of typically 1%/hr (2.8×10^{-6} /s) and had normalized base excess pore pressures $\Delta u/\sigma_v$ less than 5% in the normally consolidated stress range for that strain rate. Estimates of σ'_p were made using the strain energy method [42]. The σ'_p values plotted in Figure 16a are not adjusted for possible CRS strain rate effects. According to Mesri and Feng [43] and Mesri et al. [44], σ'_p values should be reduced by a factor of about 0.96 to obtain the equivalent end of primary consolidation σ'_p . The IL data plotted in Figure 14 results in a 24 hr σ'_p of 170 kPa versus the CRS σ'_p of 210 kPa. This gives a ratio of $\sigma'_{p,CRS}/\sigma'_{p,24hr}$ equal to 1.24 which is similar to the typical value of 1.25 reported by Leroueil [45] for a variety of clays.

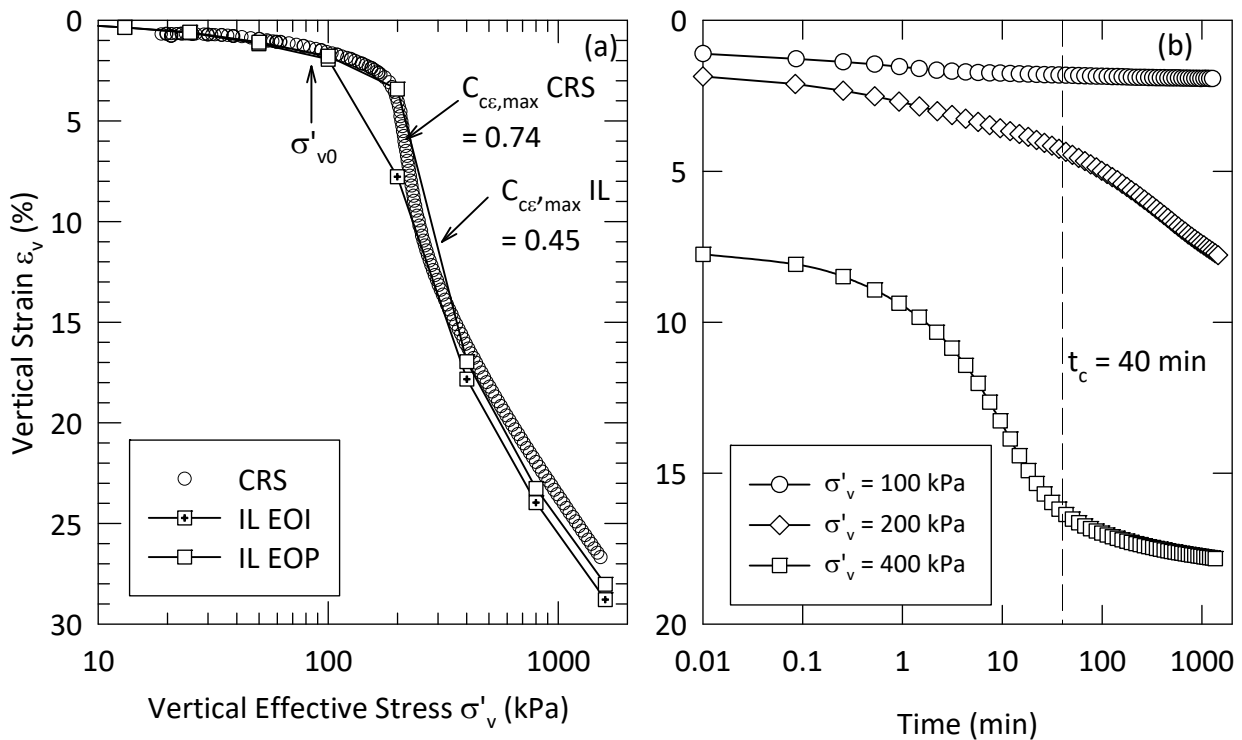


Figure 15. a) Comparison between CRS and IL data for tests conducted on same block sample ($z = 7.0$ m), b) example deformation time curves for the IL test plotted in part (a) (modified from [31]).

The σ'_p data (Figure 16a) provide evidence of a stiff crust from 4 m to 5 m depth. Within the soft clay unit (6 m to 10 m), σ'_p is approximately constant at about 210 kPa, and the corresponding OCR decreases from about 3.0 to 2.2 over this depth interval (Figure 16b). A constant σ'_p suggests possible cementation as a preconsolidation mechanism [46]. Also plotted in Figure 16a are interpreted σ'_p from CPTU data using the correlation $\sigma'_p = k(q_t - \sigma_{v0})$. A typical literature value of $k = 0.33$ was used [47,48], which agrees well with CRS data from 6 m to 8 m depth, but not well within the crust and deeper than 8 m.

Figure 16c plots values of $(C_{ce})_{max}$ and the recompression index (C_{re} ; using a scale of $10C_{re}$) versus depth. C_{re} values were determined as the slope of a line constructed through the ε_v - $\log\sigma'_v$ data

beyond σ'_{v0} that formed a straight line. C_{re} values are within the narrow range of 0.020 to 0.028. The ratio $C_{re}/C_{ce,max}$ averages 0.11 within the crust (above 6 m), while the ratio $C_{re}/C_{ce,max}$ averages 0.04 within the soft clay unit. These ratios are within the typical range of 0.02 to 0.20 [41], where the low value of 0.04 for the soft clay unit is common for that of highly structured and bonded soft clays.

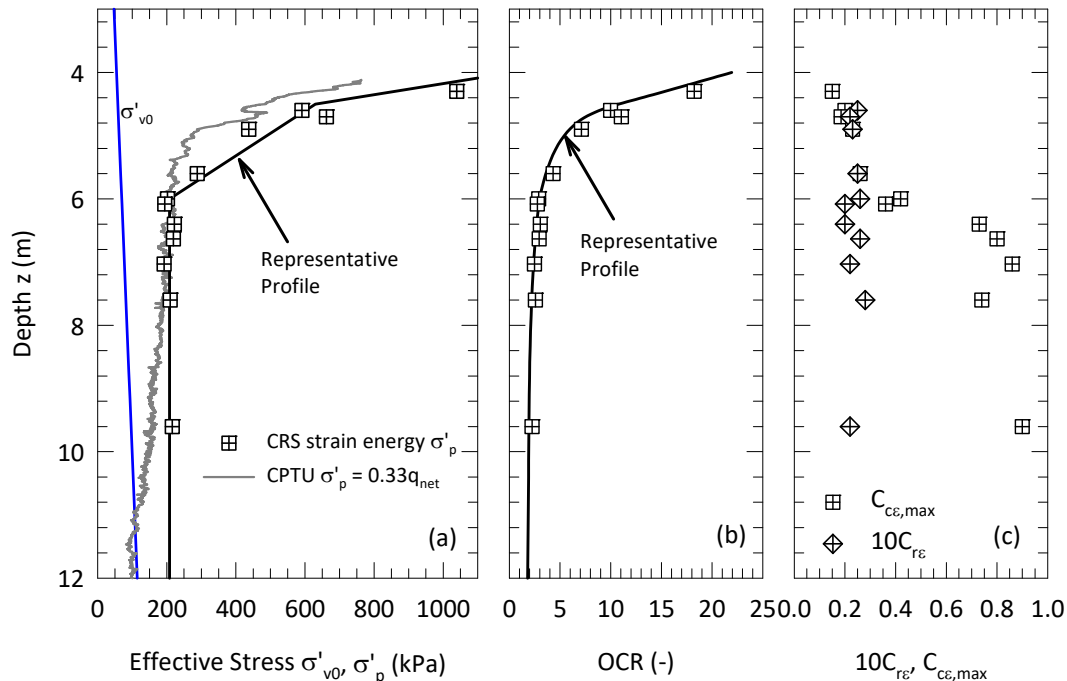


Figure 16. Newbury BBC stress history based on Sherbrooke block specimens: a) strain energy σ'_p from CRS and CPTU, b) CRS OCR, and c) recompression and maximum compression ratios.

As part of the undrained shear strength test program (Section 5.4), a K_0 consolidated triaxial compression test was conducted to an axial vertical effective stress well into the normally consolidated stress range using the approach of Menzies [49]. The resulting measured ratio of $K_0 = \sigma'_h/\sigma'_v$ for the OCR = 1 state of stress was 0.55. Following Mesri and Hayat [50], Equation 1 estimates the relationship between K_0 and OCR for the soft clay unit:

$$K_0 = 0.55(\text{OCR})^{0.45} \quad (1)$$

5.3. Coefficient of consolidation and hydraulic conductivity

Coefficient of vertical consolidation, c_v , and vertical hydraulic conductivity, k_v , were interpreted from measured CRS data using the methods of Wissa et al. [51], Sandbækken et al. [52] and ASTM D4186 [11]. Values of c_v for the soft clay unit depends significantly on stress level relative to σ'_p as shown for example in Figure 14c. Figure 17a plots three sets of c_v values: at approximately σ'_{v0} , the minimum value $(c_v)_{min}$, and at $5\sigma'_p$. For the soft clay unit below 5 m, c_v at σ'_{v0} is greater than $10 \text{ m}^2/\text{yr}$, decreases significantly as loading continues up to and just beyond σ'_p to a minimum value averaging $1.3 \text{ m}^2/\text{yr}$ (which typically occurs around $\sigma'_v = 1.1$ to $1.3\sigma'_p$), and then progressively increases (e.g., Figure 14c) to an average of $5.6 \text{ m}^2/\text{yr}$ as σ'_v approaches $5\sigma'_p$. This latter c_v value is reasonable for

normally consolidated clays with a w_L of 47 [41] based on estimates from direct measurement of hydraulic conductivity or field settlement records. Vertical hydraulic conductivity k_{v0} at σ'_{v0} was estimated from an extrapolation to e_0 of the straight line portion of the calculated e - $\log k_v$ CRS data plot. Values of k_{v0} average 1.1×10^{-9} m/s (Figure 17b) and the corresponding value of $C_k = \Delta e / \Delta \log k_v$ averages 0.50 (Figure 17c) for the soft clay unit, both of which are in the range reported for soft clays [41]. Furthermore, C_k is well estimated using e_0 [53], and values for the soft clay unit are within the narrow range of $C_k = 0.38e_0$ to $0.40e_0$. These c_v and k_v values are likely to be the lower bound, since they were determined using small CRS specimens. No data are available for tests that involved a larger volume of soil, e.g., in situ slug tests conducted in open standpipe piezometers. Larger scale in situ values may be greater, especially in the crust where macro-features such as small fissures can be induced by desiccation. Laboratory measured values are for vertical flow only. Reported k_h/k_v values equal 1.5 ± 0.5 for soft BBC at Saugus, MA based on laboratory falling head and CRS tests on horizontally oriented specimens [54]. Similarly, the Newbury BBC deposit likely has micro layering, especially below 14 m (CPTU data in Figure 9), which would yield higher k_h values.

The rate of secondary compression $C_{\alpha\varepsilon} = \Delta\varepsilon / \Delta \log t$ for the soft clay unit correlates well with $C_{c\varepsilon}$ determined from several IL oedometer tests conducted on the Sherbrooke block sample specimens. $C_{c\varepsilon}$ was estimated for multiple load increments using the first log cycle of time beyond the end of primary consolidation using Casagrande construction. The ratio $C_{\alpha\varepsilon} / C_{c\varepsilon}$ averages 0.03 for recompression and virgin compression, which is on the low end of that for most inorganic clays and silts (0.04 ± 0.01) [41].

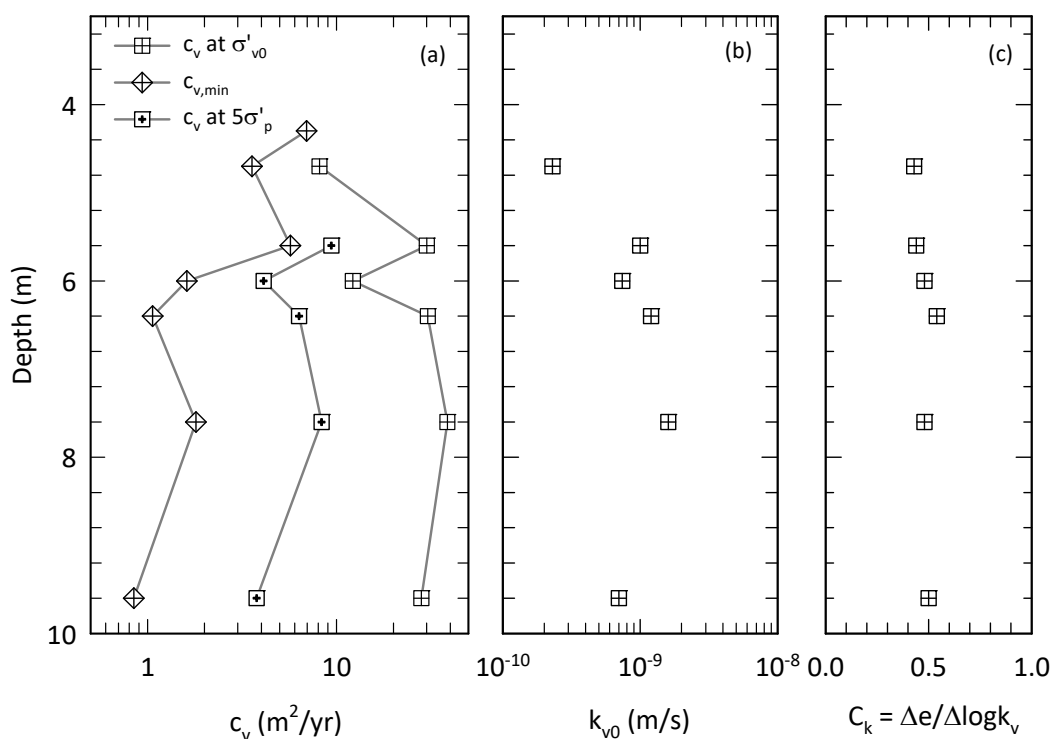


Figure 17. Newbury BBC values of a) vertical coefficient of consolidation c_v , b) vertical hydraulic conductivity k_{v0} , and c) hydraulic conductivity coefficient C_k .

5.4. Undrained shear strength

Advanced laboratory tests conducted on Sherbrook block sample specimens consisted of anisotropically consolidated undrained triaxial compression (CAUC) and undrained direct simple shear (DSS) tests. Triaxial tests were conducted using computer controlled stress path cell systems and the methods described by Germaine and Ladd [55] and Lacasse and Berre [56]. The CAUC specimens were consolidated using the Recompression method [31,57] to the best estimate of the in situ effective stress state with $\sigma'_{vc} = \sigma'_{v0}$ and $\sigma'_{hc} = \sigma'_{h0} = K_0\sigma'_{v0}$. K_0 was estimated using Equation 1 and the representative stress history profile in Figure 16. DSS tests were performed using a Geonor device with a wire reinforced membrane following the procedures of Bjerrum and Landva [58], DeGroot et al. [59], and ASTM D6528 [11]. The DSS specimens were initially preloaded to $\sigma'_v \approx 0.7\sigma'_p$ prior to unloading to $\sigma'_{vc} = \sigma'_{v0}$ using σ'_p estimated from the CRS tests conducted on the block samples. This was to lock in a reasonable σ'_{hc} for an overconsolidated state, since σ'_{hc} cannot be directly controlled in the Geonor device. A suite of K_0 consolidated undrained triaxial compression (CK₀UC) and DSS tests were also performed using the SHANSEP method [31,60]. These specimens were loaded to a normally consolidated state of stress by targeting an axial strain of approximately 10% for the CK₀UC specimens and approximately 15% for the DSS specimens. SHANSEP OCR > 1 tests were subsequently unloaded from these states to the target OCR. Lastly, a complementary set of strength index tests were performed on the samples including unconsolidated undrained triaxial compression (UUC), fall cone (FC), and torvane (TV).

The CAUC specimens had $\Delta e/e_0$ at σ'_{v0} values of less than 0.03, rating the samples “very good to excellent” as per Lunne et al. [40]. The undrained shear behavior plotted in Figure 18 shows the brittle nature of the soft clay unit, which has a low axial strain at peak shear stress followed by significant strain softening. Specimens initially developed some positive shear induced pore pressure, but suddenly decreased at the peak shear stress, exhibiting dilative behavior. Post peak shear stress, the soil's brittle nature, rapid destructuring, and reduction in pore pressure caused the effective stress path to loop backwards and converge towards a maximum obliquity state of stress. DSS specimens likewise show a tendency towards dilative behavior prior to reaching the peak shear resistance, although the brittleness manifest in the stress plot is not as noticeable in the DSS mode of shear (Figure 19).

Figure 20a plots the undrained shear strength data versus depth. The CAUC and DSS s_u values are essentially constant with depth in the soft clay unit, with average values of $s_{uC} = 48$ kPa and $s_{uD} = 34$ kPa. The constant s_u depth profiles are similar to those of σ'_p (Figure 16a). These average values correspond to an undrained shear strength anisotropy ratio $K_s = s_{uD}/s_{uC} = 0.72$. Also plotted in Figure 20a are the estimated s_u profiles based on the SHANSEP testing, which resulted in the following equations for OCR < 5 (Figure 21a):

$$s_{uC} = S\sigma'_{v0}(\text{OCR})^m = 0.28\sigma'_{v0}(\text{OCR})^{0.60} \quad (2)$$

$$s_{uD} = 0.17\sigma'_{v0}(\text{OCR})^{0.74} \quad (3)$$

where $S = s_u/\sigma'_{v0}$ for OCR = 1 and m equals increase in s_u with OCR. Equations 2 and 3 were used together with the representative stress history profile in Figure 16 to produce the SHANSEP s_u profiles in Figure 20a. For both modes of shear, the SHANSEP s_u values for the soft clay unit below 6 m are on average about twenty percent less than the Recompression test values. The SHANSEP method is generally not recommended for sensitive clays such as Newbury BBC, as preshear

consolidation causes destructuring, although use of the SHANSEP method will result in lower, i.e., so-called conservative, s_u values [31].

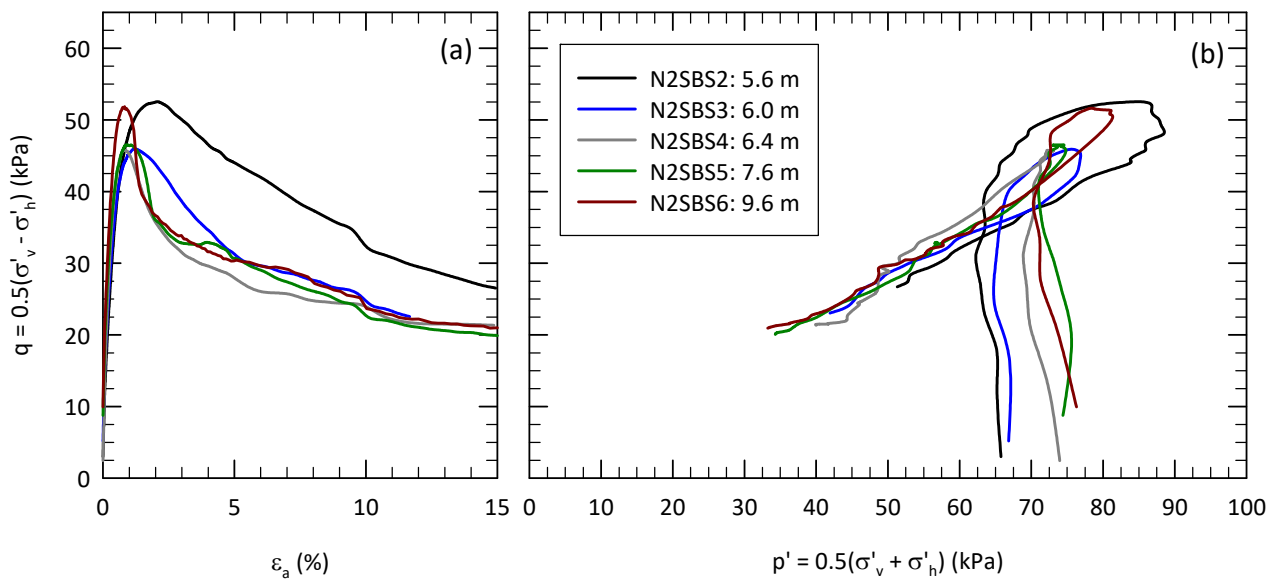


Figure 18. Newbury BBC Recompression CAUC behavior for Sherbrooke block samples a) stress-strain and b) effective stress path.

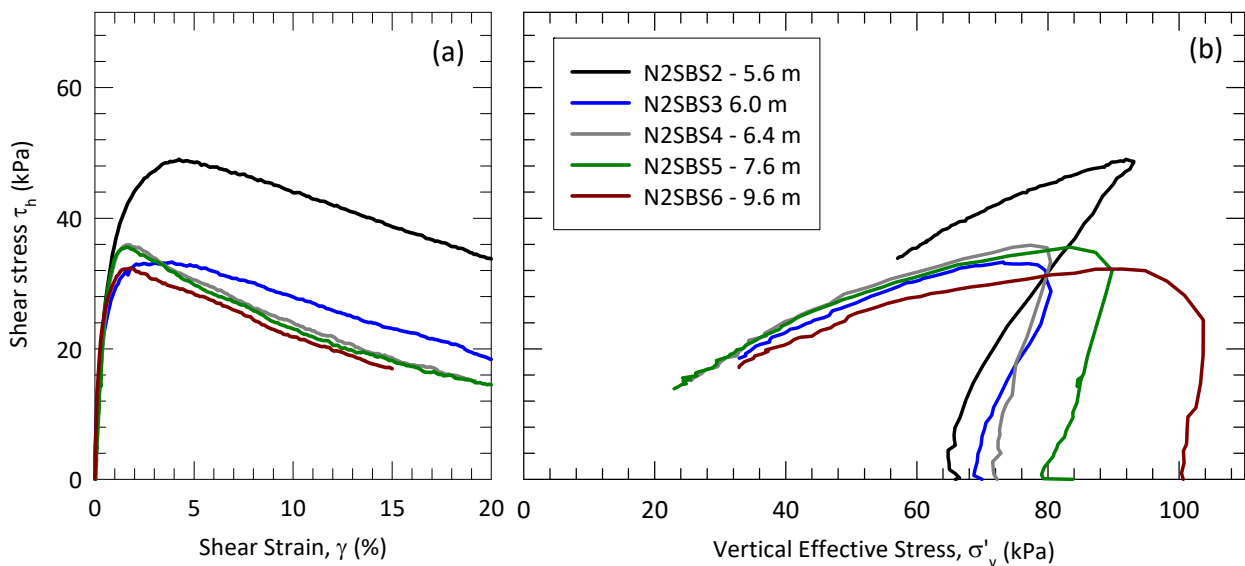


Figure 19. Newbury BBC Recompression DSS behavior for Sherbrooke block samples a) stress-strain and b) shear stress-vertical effective stress plot.

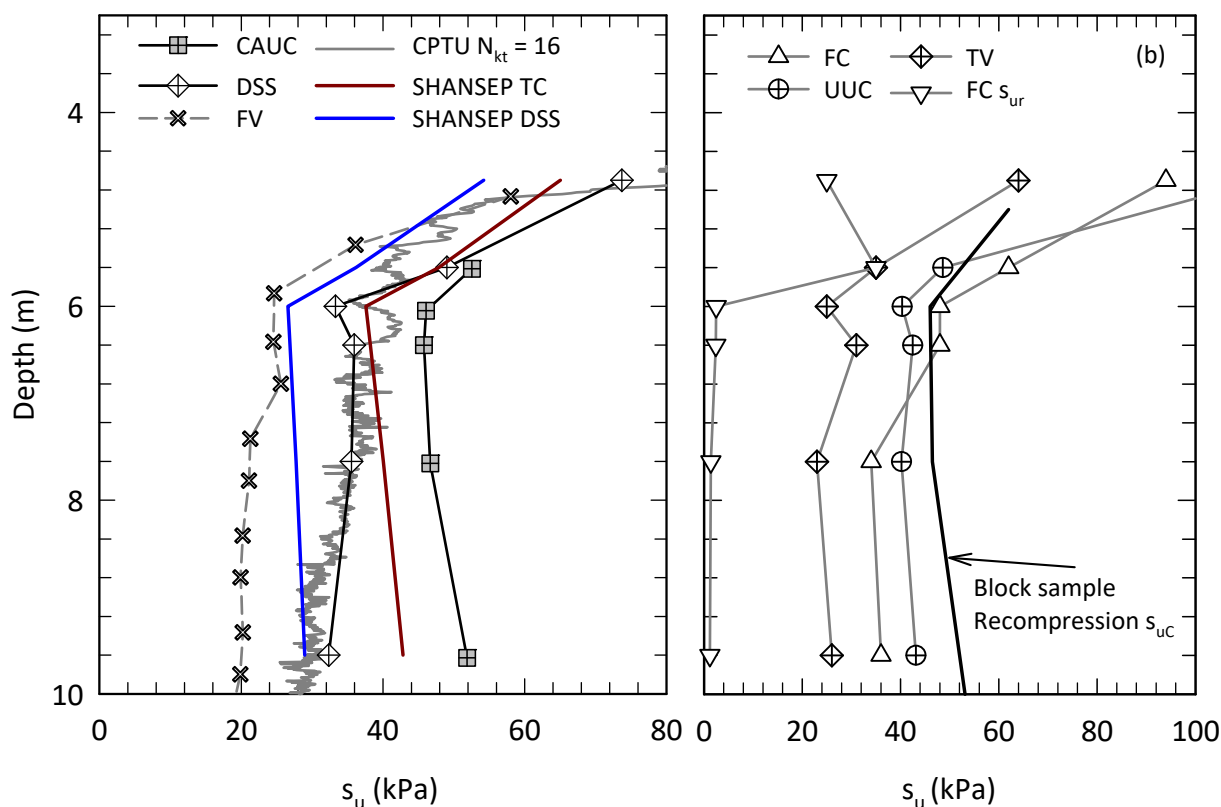


Figure 20. Newbury BBC undrained shear strength profiles from a) CAUC/CK₀UC and DSS tests on Sherbrooke block samples plus CPTU and FV and b) strength index tests.

Also plotted in Figure 20a is an interpretation of the CPTU data using $s_u = (q_t - \sigma_{v0})/N_{kt}$, where a typical literature value of $N_{kt} = 16$ was used to represent the average ($s_{u,ave}$) undrained shear strength [47,61]. The data compare favorably with the Recompression DSS data, which is reasonable given that the DSS mode of shear most closely matches $s_{u,ave}$ for most soft clays (e.g., [31]). The FV s_{uFV} values plotted in Figure 20a, depth averaged from the three soundings plotted in Figure 12, are very low. Figure 21b plots the normalized field vane strengths s_{uFV}/σ'_{v0} versus OCR as determined from the interpreted stress history data (Figure 16). The trend in the data is typical of that found for other clays (e.g., [41]) and a regression fit for $OCR < \text{five}$ gives $s_{uFV}/\sigma'_{v0} = 0.10(OCR)^{1.00}$ or simply $s_{uFV} = 0.10\sigma'_p$. The value of 1.0 for the OCR exponent is consistent with that presented by Terzaghi et al. [41] for FV data from several soft clay sites. The s_u/σ'_{v0} coefficient for $OCR = 1$ of 0.10 is very low, and it has not been determined why such low s_u values were obtained from FV tests.

Index test s_u values plotted in Figure 20b show similar depth trends as CAUC and DSS s_u data, but lower values relative to measured s_{uC} . Below 6 m, average s_u ratios are $s_{uUUC}/s_{uC} = 0.87$, $s_{uFC}/s_{uC} = 0.87$, and $s_{uTV}/s_{uC} = 0.55$. Index strengths for low OCR soft clays are often lower to much lower than CAUC strengths, especially for poor quality samples (e.g., [31]). In this case, however, the UUC and FC strengths are relatively close to that of CAUC strengths, likely from the combination of high quality samples and fast shear rates for the UUC and FC tests that to some degree compensate for the unconsolidated state of the samples during index testing. The FC sensitivity values range from 20 to 30, which is broadly similar to field vane measured sensitivities (Figure 12b).

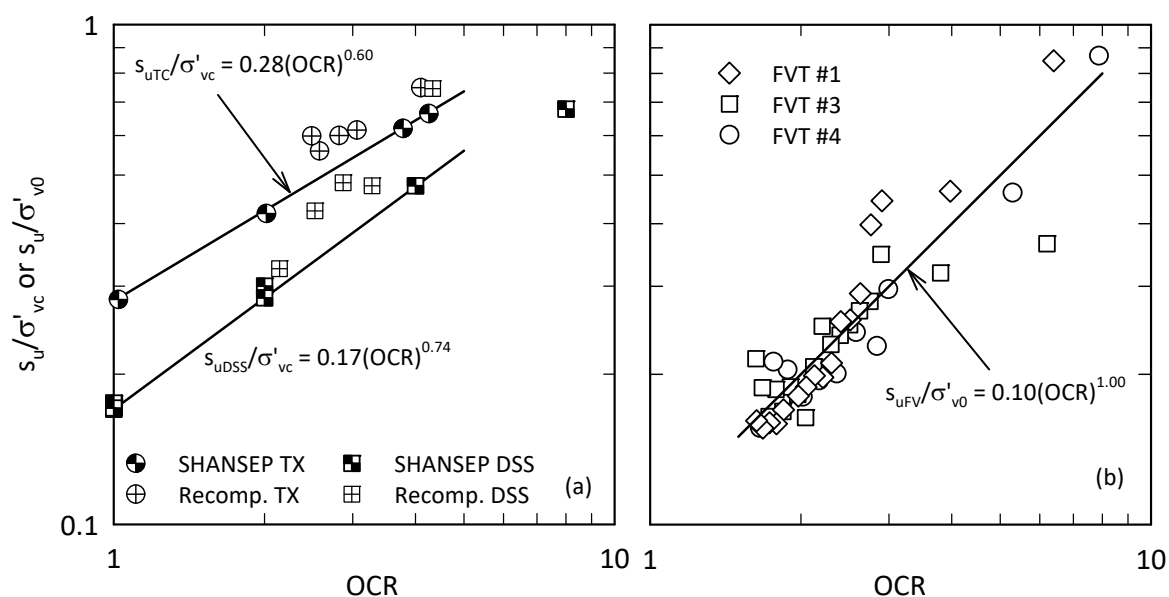


Figure 21. Newbury BBC a) comparison of normalized undrained shear strength versus OCR from Recompression and SHANSEP tests on Sherbrooke block samples and b) normalized field vane undrained strength versus OCR.

5.5. Sample disturbance

5.5.1. Influence of sampler and drilling procedure

Two different drilling methods together with four different samplers were deployed at the Newbury, MA site to study the influence of sampling variations on sample quality. Table 4 lists the combination of methods used. Sherbrooke block sampling with a barite weighted drilling mud was selected with anticipation that these procedures would result in the best quality samples. The modified Shelby tube with a fixed piston was selected to study its potential to collect tube samples of quality near to or equal to the Sherbrooke block samples. The Shelby tubes used were manufacturer supplied standard U.S. practice tubes [11] with slight modification that included removal of the approximately 5 mm of the tubes to create a zero inside clearance ratio (ICR) followed by lathe machining of the new end to have a sharper cutting angle of approximately 10° . Such a geometry used in combination with a weighted drilling mud is recommended as best practice procedures for undisturbed tube sampling of soft clays (e.g., [62–65]). The hollow stem auger method without drilling mud and use of a standard Shelby tube with a free-floating piston was also intentionally selected, as this is sometimes seen in U.S. practice. The thick walled standard penetration test (SPT) split spoon sampler was used in anticipation that this would result in poor quality samples and serve as an opposite benchmark to that of the Sherbrooke block samples. More details on the sampler geometries and drilling methods are given in Landon et al. [15].

Figures 22 and 23 present examples of the differences in the measured 1-D consolidation and CAUC triaxial test behavior for specimens obtained from the different sampling methods. Figure 24 plots profiles of $\Delta e/e_0$ at σ'_{v0} and strain energy σ'_p estimates, Figure 25a plots σ'_p vs $\Delta e/e_0$, and Figure 26 plots various s_u profiles for the different sampling methods. As expected, the Sherbrooke block

samples overall had the best quality and the SPT the poorest. These data provide classic examples of the detrimental effect of sample disturbance on 1-D compression and shear behavior of a soft clay with significant reductions in σ'_p and s_{uC} with increasing disturbance, as reported by others (e.g., [40]). Some noteworthy observations from this data set are: 1) fixed piston samples with modified tube geometry deployed in a borehole with a weighted drilling mud produce σ'_p results similar to those from block samples, but not similar CAUC strengths or shear behavior; 2) in some cases, the free piston samples collected without drilling mud also had a good quality sample rating, but this appears random, as some samples were certainly of poorer quality; 3) s_{uD} is less influenced by sample quality than s_{uC} , as also reported by Lunne et al. [40]; 4) UUC tests conducted on high quality samples give s_{uUUC} values close to s_{uC} ($s_{uUUC}/s_{uC} = 0.87$) (Section 5.4, Figure 20), and presumably the potential decrease in s_{uUUC} due to lack of reconsolidation to the in situ stress state is partly compensated by strain rate effects from the fast shear rate used in UUC testing.

Table 4. Drilling and sampling methods used at the Newbury, MA BBC site.

| Borehole Advancement | Drilling Mud | Sampler | Sampler Geometry |
|-------------------------------|--------------------------|---|---|
| Hollow Stem Auger | No mud | 75 mm OD SPT sampler with 6" liners | 60° edge angle, $t = 15$ mm, 60% AR, 0 ICR |
| Hollow Stem Auger | No mud | Standard 76 mm OD Shelby tube with free piston | $\approx 44^\circ$ † edge angle, $t = 1.6$ mm, 12% AR, 3% ICR |
| Mud Rotary “best practice” | Drilling mud with barite | Modified 76 mm OD Shelby tube with fixed piston sampler | 10° edge angle, $t = 1.6$ mm, 9% AR, 0 ICR |
| Auger | Drilling mud with barite | Sherbrooke Block Sampler | n/a |

Notes: OD = outside diameter, t = wall thickness, AR = area ratio, ICR = inside clearance ratio, †angle approximate as cutting edge is curved

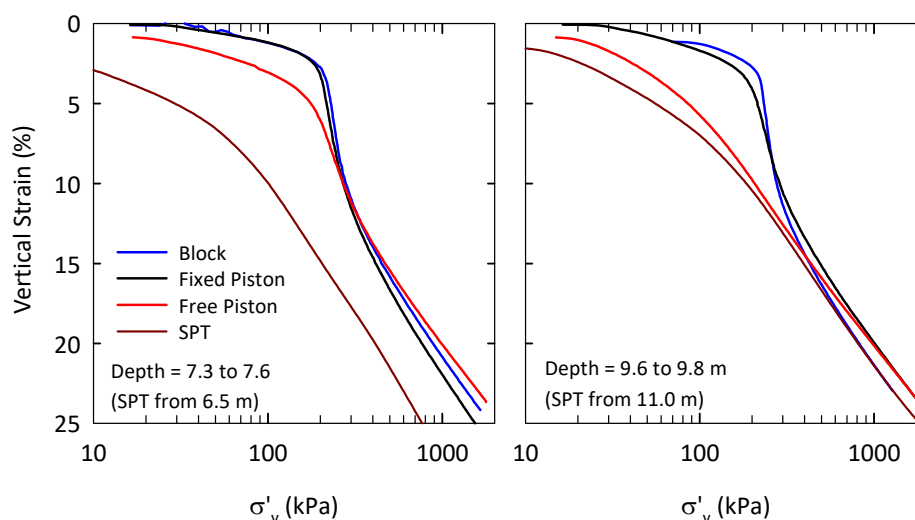


Figure 22. Influence of different sampling methods on CRS behavior of Newbury BBC, a) depth interval 7.3 to 7.6 m and b) depth interval 9.6 to 9.8 m.

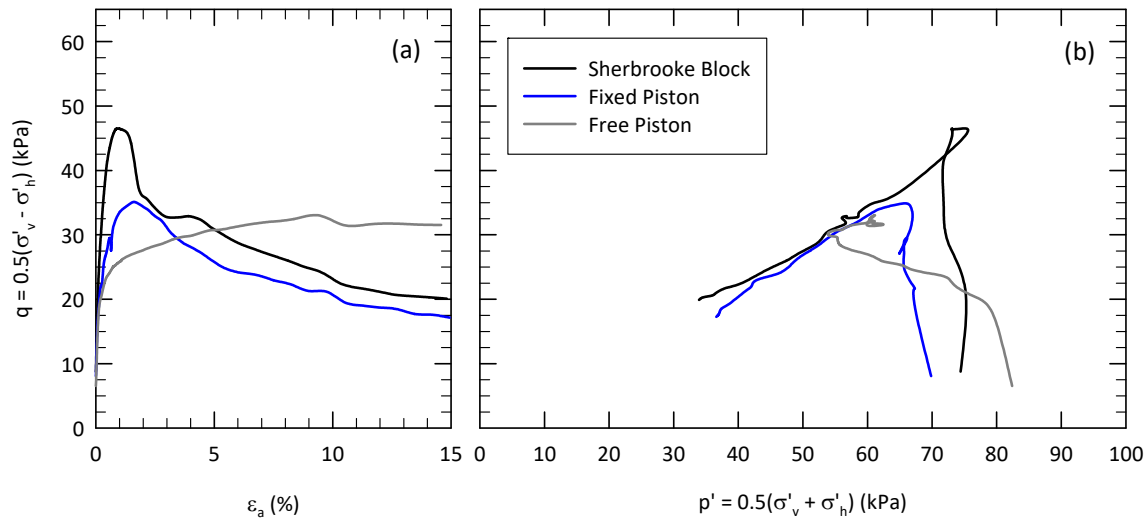


Figure 23. Influence of different sampling methods on Recompression CAUC behavior of Newbury BBC from depth interval 7.3 to 7.6 m a) stress-strain and b) effective stress path.

5.5.2. Non-destructive measures of sample quality

Two non-destructive measures of sample quality, shear wave velocity and suction, were investigated at the Newbury site. Landon [4] and Landon et al. [15] describe the shear wave velocity equipment, measurement procedures, and results, while Poirier [2] and Poirier and DeGroot [16] describe the same for suction measurements. Shear wave velocity was measured on the samples in the field almost immediately after sampling using a bender element equipped testing jig. The measurements were taken over the full length of the Sherbrooke block samples and over a short, approximately 7 cm, section cut from the tube samples. Sample suction was measured using a suction probe placed directly on the surface of the block samples and the same cut section of the tube samples used for the shear wave velocity measurement. Figure 27 plots the shear wave velocity (V_{vh}) and suction (u_r) values versus depth for samples collected using the four different sampling methods listed in Table 4. The representative shear wave velocity profile determined from the SCPTU testing (Figure 11a) is plotted for reference in Figure 27a. Likewise, a reference line equal to $0.2\sigma'_{v0}$ suggested by Tanaka et al. [66] to be an indication of a high quality sample for normally consolidated to lightly overconsolidated clays is plotted in Figure 27b. Also included in Figure 27 are values of V_{vh} and u_r measured on samples completely remolded in the laboratory.

All measured V_{vh} values are less than that of the SCPTU. The range in measured values is significant, with the block sample values being the largest and the SPT samples the lowest. A similar trend among the samplers is shown in the u_r data, albeit with more scatter. High quality block and fixed piston samples plot around the $0.2\sigma'_{v0}$ line, while poor quality SPT samples and remolded specimens had zero or near zero suction. Normalized V_{vh}/V_{SCPTU} and u_r/σ'_{v0} data are plotted versus σ'_p in Figure 25b and 25c. The trend of a decrease in σ'_p with an increase in $\Delta e/e_0$ (Figure 25a) is similarly tracked by a decrease in both V_{vh}/V_{SCPTU} and u_r/σ'_{v0} . These results indicate the efficacy of nondestructive sample quality measurements in assessing quality. More research is needed for a wide array of soft clays before a definitive sample quality criteria can be implemented in practice. Examples of similar data for other clays are given in Hight et al. [67] and Donohue and Long [68].

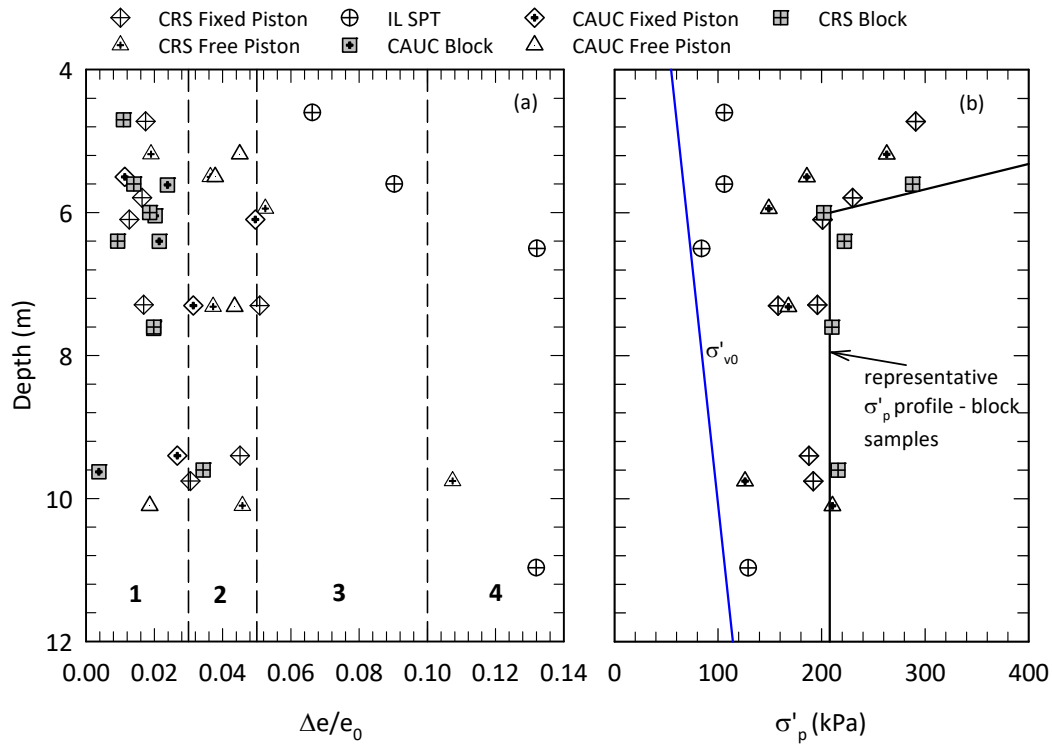


Figure 24. Newbury BBC a) CRS/IL and CAUC sample quality versus depth and b) σ'_p data from consolidation tests on different sampling methods (where numbers 1–4 indicate sample quality designated using Lunne et al. [39], with 1 being “very good to excellent” and 4 being “very poor”).

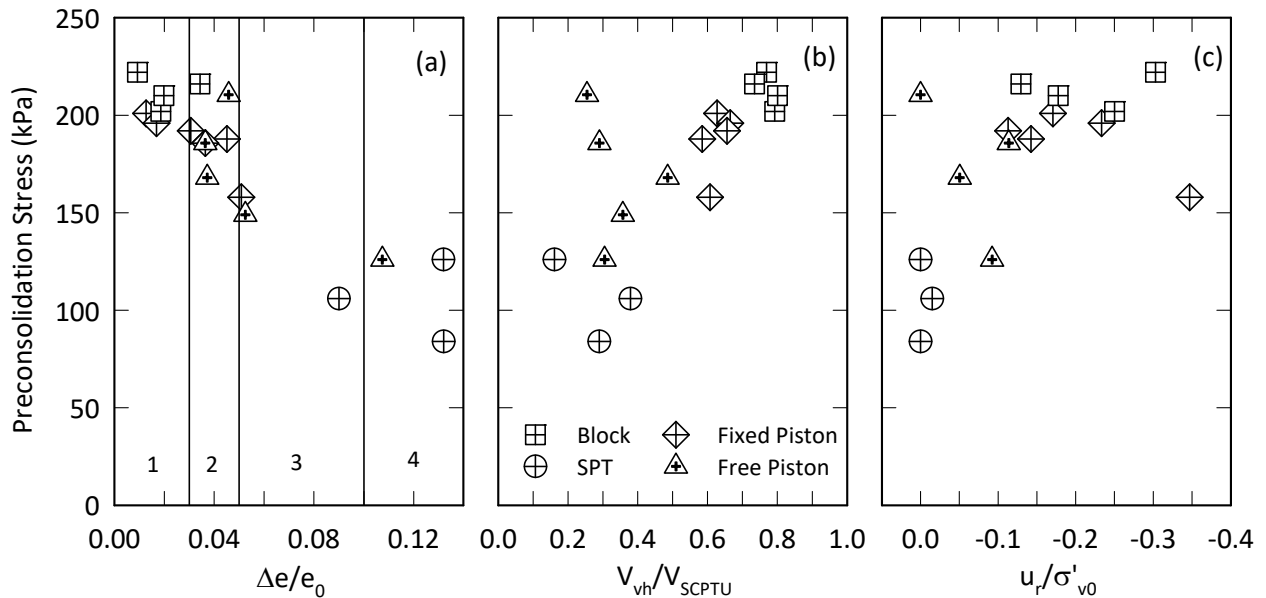


Figure 25. Newbury BBC correlation between σ'_p and measures of sample quality a) $\Delta e/e_0$, b) normalized shear wave velocity, and c) normalized suction.

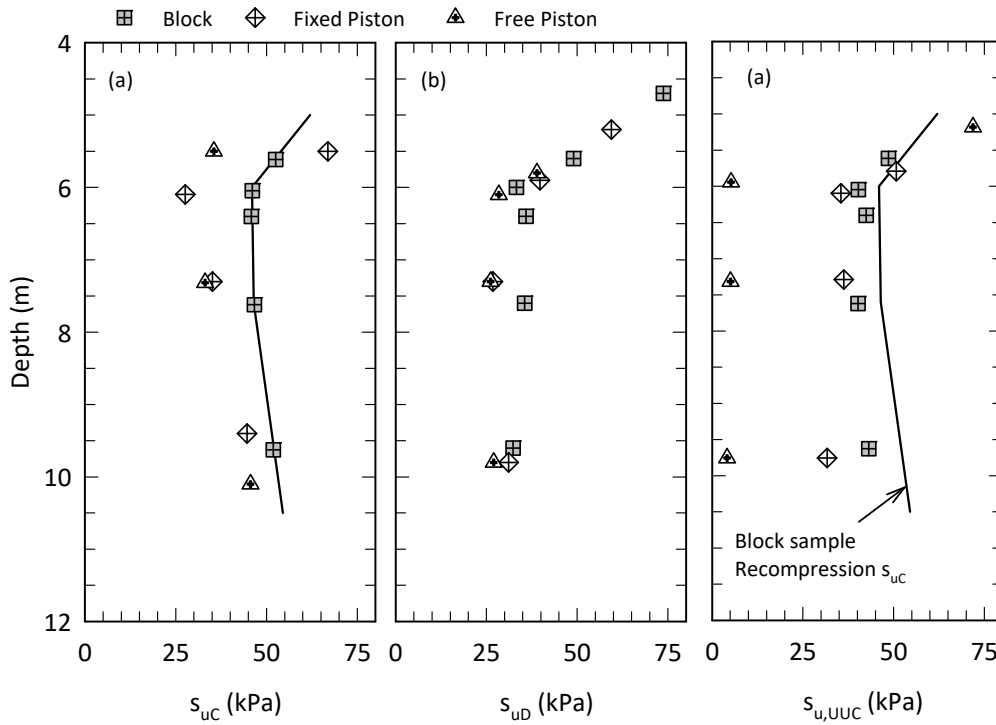


Figure 26. Newbury BBC measurements of undrained shear strength for different sampling methods, a) Recompression CAUC, b) Recompression DSS, and c) unconsolidated undrained triaxial compression.

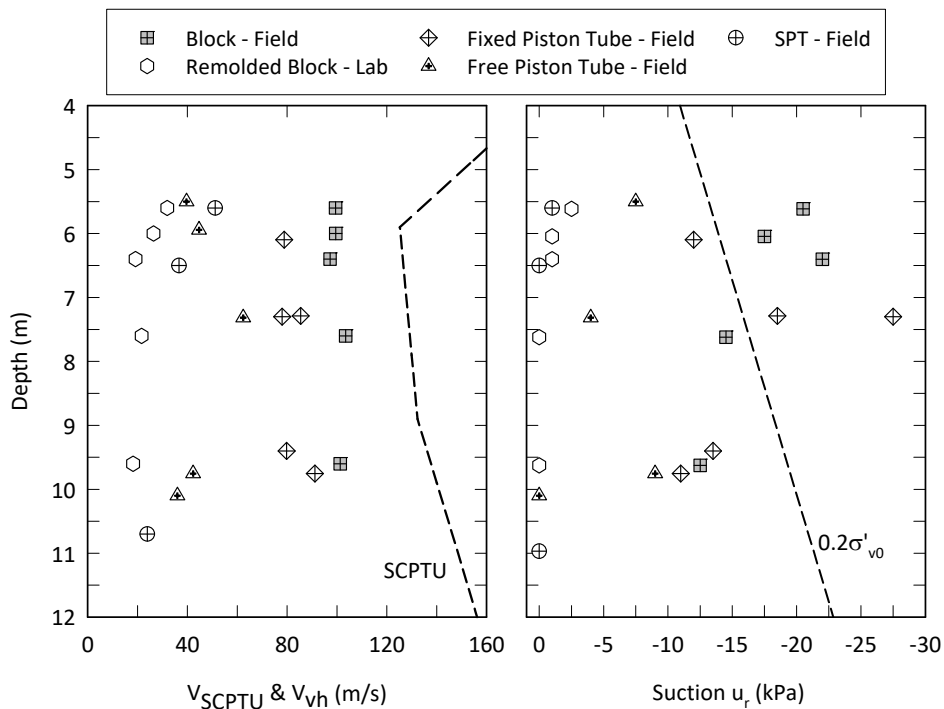


Figure 27. Newbury BBC depth profiles of measurement of sample quality for different sampling methods a) shear wave velocity and b) suction.

5.6. Comparison with published data on intact BBC

There has been extensive testing conducted at MIT on reconstituted natural BBC, but less so on intact samples. While numerous projects have and continue to be constructed on and in BBC in the greater Boston area, site investigation data are often not available in the published literature or did not include a comprehensive suite of in situ and advanced laboratory tests conducted on good quality samples. Some notable recent exceptions include Berman et al. [69] for deep excavations on the MIT campus in Cambridge, MA, Ladd et al. [70] on settlement behavior of a test embankment in Saugus MA, and Ladd et al. [71] for the Central Artery/Third Harbor Tunnel project in Boston. Mesri and Ali [22] also conducted an extensive series of 1-D consolidation and consolidated undrained triaxial tests on OCR = 3 block samples of BBC that were carved from a deep excavation in Boston.

The BBC deposit studied by Berman et al. [69], Ladd et al. [70], and Ladd et al. [71] is much thicker than that at the Newbury, MA site and includes a crust approximately 15 m thick compared to the thin 2 m crust at the Newbury. This is further confirmed in the profiles in Figure 3. Below the crust, the OCR in Boston is generally less than 2, which is lower than that measured at Newbury, although the Boston results are measured from a greater depth. Furthermore, the deep Boston deposit appears to be less sensitive based on indirect evidence from liquidity index I_L values. Boston I_L values range from 0.5 to 0.8, compared to greater than 1.0 at Newbury. Values of $K_{0,NC}$ based primarily on measurements from the K_0 consolidation phase of triaxial tests are the same: 0.55 for Newbury, 0.56 from Berman et al. [70], 0.55 from Ladd et al. [71], and 0.56 from Mesri and Ali [22].

Recompression and SHANSEP undrained shear strength data from other studies are compared in Table 5 with that for the Newbury site. Triaxial test data are for both compression (TC) and extension (TE). Other than TE, S-values (Eqs 2 and 3) are similar for Recompression and SHANSEP methods. Values of m tend to be larger for the Recompression method, with a net effect that SHANSEP s_u values are generally lower for all modes of shear, as expected [31]. Also, m -values (Eqs 2 and 3) generally increase from TC to DSS to TE, meaning that s_u anisotropy decreases with an increase in OCR as reported by others [60,72,73]. Differences in m -values are more important for the Boston area sites, as the overconsolidated crust is much thicker. The similarity among the data is valuable for engineering practice; the values can be used as being generally representative of BBC for feasibility studies, preliminary design and also as a check of data is being obtained at new sites.

Table 5. Comparison of normalized undrained shear strength parameters for several BBC sites.

| Shear Mode | Recompression | | SHANSEP | | Location | Reference |
|--------------------|---------------|-------|---------|------|----------------|------------|
| | S | m | S | m | | |
| CAUC, | 0.29 | 0.70 | 0.28 | 0.60 | Newbury, MA | this paper |
| CK ₀ UC | 0.30 | 0.68 | 0.28 | 0.68 | City of Boston | [71] |
| | 0.28 | 0.73+ | 0.28 | - | City of Boston | [22] |
| DSS | 0.16 | 1.00 | 0.17 | 0.74 | Newbury, MA | this paper |
| | - | - | 0.18 | 0.68 | City of Boston | [71] |
| | - | - | 0.19 | 0.75 | Saugus, MA | [74] |
| CAUE, | 0.14 | 0.98 | 0.14 | 0.83 | City of Boston | [71] |
| CK ₀ UE | 0.17 | 0.83+ | 0.17 | - | City of Boston | [22] |

Note: CAUC/CAUE for Recompression, CK₀UC/CK₀UE for SHANSEP, +for tests consolidated in range of σ'_{v0} and σ'_p .

6. Engineering challenges

Boston Blue Clay is widely distributed over a large geographic region and frequently presents engineering design and construction challenges. This is particularly the case in the major metropolitan City of Boston within which there has been significant infrastructure development in the past few decades. Such projects involving BBC have included new tunnels, relocation of a major interstate freeway to below ground, and foundations and deep excavation support systems for numerous high rise buildings. The complex and highly variable geologic history of BBC means that there can be significant spatial variations in the presence of the deposit and its geotechnical engineering properties. Primary characterization items of interest early on in a proposed project is the presence and thickness of the deposit, the thickness and stiffness of the crust, and whether an infrastructure project will be founded within the soft clay unit. The results presented in this paper show that for BBC at the Newbury site, the CPTU provides valuable stratigraphic information, empirical correlation to engineering properties and that best practice drilling and sampling methods (Table 4) are essential to measure accurate laboratory stress-strain-strength behavior. Depending on project specific design concepts, proper attention to this in the site characterization program for new projects can result in cost savings.

The data presented in this paper provides a valuable frame of reference for other BBC deposits with similar basic index and classification properties (Tables 2 and 3). While the Newbury BBC deposit is thinner and more sensitive than that encountered within and close to Boston [22,71] the triaxial and DSS undrained shear strength – overconsolidation ratio parameters are similar (Table 5). Some examples of completed major infrastructure projects that also provide a valuable reference for BBC properties and performance data include tunnels and underground construction [10,75], deep excavation support systems [10,75–79], deep foundations [10,80,81], embankment stability and settlement [70], and ground improvement [82]. Experience from these projects emphasize the importance of high quality geotechnical site investigations, similar to that reported herein for the Newbury BBC site, and site history analyses for complex projects.

For example, finite element analyses (FEA) of excavations showed the importance of the underlying BBC on predicted wall deflection and ground movement, especially for deep excavations embedded in BBC [76]. Other findings [77–79] found that pre-construction FEA models could not provide reliable predictions of soil deformations to the accuracy required by design engineers. Many of the pre-construction models relied on general or average soil properties for BBC or simplified models (e.g., 2D instead of 3D). Those performing the post-construction analyses found that the pre-construction analyses were limited by insufficient site investigation and a lack of site-specific BBC soil property data. Another example is the Central Artery/Tunnel (i.e., CA/T or the “Big Dig”) project which was a large public works project that included replacing an elevated highway and building a highway tunnel system under downtown Boston and the Boston Harbor. Many components of the project required minimizing construction-related impacts to nearby structures and utilities due to the densely developed and populated area and the presence of the compressible and soft, deeper BBC deposit. Early on in the project the consequence of BBC on construction performance was not well developed and early cut and cover excavation work on the western approach to an immersed tube tunnel under Boston Harbor [75] resulted in excessive settlement of BBC due to dewatering. As work progressed on the CA/T project, consolidation settlement due to dewatering had to be mitigated by staging the excavations and reducing the groundwater drawdown,

even though this impacted project schedule and cost. Likewise, many modern structures in Boston are founded on deep pile foundations and located adjacent to older, low-rise buildings (some historically significant) supported by short wooden piles or caissons bearing in the upper crust in the BBC. Due to the lack of available space, more cost-effective alternative foundation types are limited for the loading required by most modern structures, and piles or pre-consolidation are required. However, these are not without challenges such as ground heave during installation which can result in distress or damage to adjacent buildings or surface features, and is most pronounced within saturated, insensitive clay soils [80]. The pile driving induced heave is generally temporary and often followed by net settlement as excess pore pressures generated during driving dissipate and the BBC further consolidates. As such, a key factor in ground heave prediction is information from the site characterization program on the thickness and depth of BBC, its sensitivity and consolidation properties, and the presence of granular soil layers [81].

7. Conclusions

Boston Blue Clay (BBC) is a glacial marine soil that is commonly found in the greater Boston, Massachusetts, U.S. region. The thickness, stress history and soil properties can vary significantly depending on location due to differences in source material, depositional environment, and subsequent geologic history. At the Newbury, MA site, which is located 60 km north of Boston, the BBC deposit is approximately 12 m thick and includes a 2 m thick upper stiff desiccated crust. Classification and engineering properties such as consolidation and undrained shear strength were determined for the Newbury BBC using a combination of in situ testing and advanced laboratory tests conducted on high quality Sherbrooke block samples. The clay fraction is 60%, plasticity index 20, and liquidity index increases from near zero within the crust to greater than one within the soft clay unit. Engineering properties such as preconsolidation stress (σ'_p) and undrained shear strength (s_u) decrease significantly with depth within the crust, but are thereafter approximately constant with depth within the soft clay unit. The constant σ'_p of about 210 kPa within the soft clay unit corresponds to an overconsolidation ratio decreasing from approximately 3 to 2. The strength sensitivity based on field vane and fall cone testing ranges from about 20 to 30. During 1-D laboratory consolidation the soft clay undergoes significant destructuring, which corresponds to these sensitivity values. The overall 1-D consolidation and flow properties such as compressibility, hydraulic conductivity, and coefficient of consolidation are similar to that reported for other similar soft clays. The approximately constant values with depth for s_u from anisotropic consolidated triaxial compression (CAUC) and direct simple shear (DSS) Recompression tests are s_{uC} of 48 kPa and s_{uD} of 34 kPa, respectively, giving an undrained shear strength anisotropy ratio equal to 0.72. CAUC and DSS tests performed using the SHANSEP method gave s_u values approximately 20% less than corresponding Recompression values.

Fixed piston samples collected using mud rotary drilling and thin walled Shelby tubes modified to have a sharp cutting angle and zero inside clearance ratio were found to give 1-D consolidation and DSS results similar to the block samples and somewhat lower CAUC s_u values. Samples collected with a free piston Shelby tube and a thick walled SPT sampler were found to have been significantly disturbed and gave much lower σ'_p and s_u values. Non-destructive measures of sample quality conducted in the field immediately after sample collection using bender elements for shear

wave velocity and a suction probe for soil suction were found to give similar trends to the traditional measure of sample quality using volumetric change during laboratory reconsolidation.

BBC frequently presents engineering design and construction problems as the deposit is widely distributed within the greater Boston area which is a major metropolitan city within which there has been significant infrastructure development in the past few decades. The first issues of interest for any proposed project is the presence and thickness of the deposit, the thickness of the crust, and whether an infrastructure project will be founded within the soft clay unit. The BBC deposit at Newbury Massachusetts is thinner and more sensitive than that often encountered in and closer to Boston. Although the Newbury BBC triaxial and DSS s_u -OCR parameters are similar to that reported for some major site investigations conducted in Boston.

Acknowledgements

This study was primarily supported by the U.S. National Science Foundation (NSF) under Grant Nos. CMS-9812106, CMS-0219480 and OISE-0530151. Any opinions, findings, and conclusions or recommendations expressed in this paper are those of the authors and do not necessarily reflect the views of the NSF.

Conflict of interest

All authors declare no conflicts of interest in this paper.

References

1. Paikowsky SG, Chen YL (1998) Field and Laboratory Study of the Physical Characteristics and Engineering Parameters of the Subsurface at the Newbury Bridge Site. Res Rpt, Dept of Civil and Environ. Engineering, University of Massachusetts Lowell.
2. Poirier SE (2005) Evaluation of Soil Suction as an Indicator of Sample Quality for a Soft Saturated Marine Clay. PhD Thesis, University of Massachusetts Amherst.
3. Jakubowski J (2005) Use of Seismic CPTU for Site Characterization in Soft Clays. Masters of Science, University of Massachusetts Amherst.
4. Landon MM (2007) Development of Non-Destructive Sample Quality Assessment Method for Soft Clays. PhD Thesis, University of Massachusetts Amherst.
5. Ryan R (2011) Incremental Loading and Constant Rate of Strain Consolidation of Clays Using Block Samples. Master of Science Thesis, University of Massachusetts Amherst.
6. Hein CJ, Fitzgerald DM, Buynevich IV, et al. (2014) Evolution of paraglacial coasts in response to changes in fluvial sediment supply, Martini IP, Wanless HR (eds), *Sedimentary Coastal Zones from High to Low Latitudes: Similarities and Differences*, Geological Society, London, Special Publications 388, 247–280.
7. Hein CJ, FitzGerald DM, Carruthers EA, et al. (2012) Refining the model of barrier island formation along a paraglacial coast in the Gulf of Maine. *Mar Geol* 307–310: 40–57.
8. Oldale RN, Colman SM, Jones GA (1993) Radiocarbon ages from two submerged strandline features in the western Gulf of Maine and a sea-level curve for the northeastern Massachusetts Coastal Region. *Quat Res* 40: 38–45.

9. Kenney TC (1964) Sea-level movements and the geologic histories of the post-glacial marine soils at Boston, Nicolet, Ottawa, and Oslo. *Géotechnique* 14: 203–230.
10. Barosh PJ, Woodhouse D (2012) A City Upon a Hill: The Geology of the City of Boston & Surrounding Region. Civil Engineering Practice. *J Boston Soc Civ Eng Sect/ASCE* 26 & 27: 480.
11. ASTM (2005) *Annual Book of Standards*, Vol. 4.08, Soil and Rock (I): D421—D5876 and Vol. 4.09, Soil and Rock (II): D5878—latest. West Conshohocken, PA, USA.
12. Lefebvre G, Poulin C (1979) A new method of sampling in sensitive clay. *Can Geotech J* 16: 226–233.
13. DeGroot DJ, Lunne T, Sheahan TC, et al. (2003) Experience with downhole block sampling in soft clays. Proceedings 12th Panamerican Conference on Soil Mechanics and Geotechnical Engineering, Cambridge, MA, 521–526.
14. Dreimanis A (1962) Quantitative Gasometric Determination of Calcite and Dolomite by Using Chittick Apparatus. *J Sediment Petrol* 32: 520–529.
15. Landon MM, DeGroot DJ, Sheahan TC (2007) Non-Destructive sample quality assessment of a soft clay using shear wave velocity. *J Geotech Geoenvironmental Eng* 133: 424–432.
16. Poirier SE, DeGroot DJ (2010) Development of a portable probe for field and laboratory measurement of low to medium values of soil suction. *Geotech Test J* 33: 3.
17. Stone BD, Stone JR, McWeeney LJ (2004) Where the glacier met the sea: Late Quaternary geology of the northeast coast of Massachusetts from Cape Ann to Salisbury, In: Hanson L (Ed.), New England Intercollegiate Geological Conference, Salem, Massachusetts, Trip B-3, 25.
18. Schnitker D, Belknap DF, Bacchus TS, et al. (2001) Deglaciation of the Gulf of Maine, Deglacial history and relative sea-level changes, northern New England and adjacent Canada, Thomas K. Weddle, Michael J. Retelle, 9–34.
19. Ridge JS, Canwell BA, Kelly MA, et al. (2001) Atmospheric ¹⁴C chronology for late Wisconsinan deglaciation and sea-level change in eastern New England using varve and paleomagnetic records, In: Thomas K. Weddle, Michael J. Retelle, eds., *Deglacial history and relative sea-level changes, northern New England and adjacent Canada*, 171–189.
20. Kaye CA (1961) Pleistocene stratigraphy of Boston, Massachusetts. United States Geological Survey Professional Paper, 424-B, 73–76.
21. Kaye CA (1982) Bedrock, and quaternary geology of the Boston area, Massachusetts. U.S.A. *Geol Surv Am Rev Eng Geol* 5: 25–40.
22. Mesri G, Ali S (1999) Undrained shear strength of a glacial clay overconsolidated by desiccation. *Géotechnique* 49: 181–198.
23. Johnson EG (1989) Geotechnical characteristics of the Boston area. *Civ Eng Pract* 4: 53–64.
24. Hein CJ, FitzGerald DM, Barnhardt WA, et al. (2010) Onshore-offshore surficial geologic map of the Newburyport East Quadrangle, Massachusetts, State Map Preliminary Map, 1 sheet.
25. Paikowsky SG, Hajduk EL (2004) Design and construction of three instrumented test piles to examine time dependent pile capacity gain. *Geotech Test J* 27: 515–531.
26. Holtz RD, Kovacs WD, Sheahan TC (2011) *An Introduction to Geotechnical Engineering*. 2nd Edition, Pearson, New Jersey.
27. Burland JB (1990) On the compressibility and shear strength of natural clays. *Géotechnique* 40: 329–378.

28. Chandler RJ (2000) Clay sediments in depositional basins: the geotechnical cycle. *Q J Eng Geol Hydrogeol* 33: 7–39.
29. Nagaraj TS, Miura N (2001) *Soft Clay Behaviour*. A.A. Balkema Publishers, Rotterdam, Netherlands.
30. DeGroot DJ, Landon MM, Lunne T (2008) Synopsis of recommended practice for sampling and handling of soft clays to minimize sample disturbance. Proceedings of 3rd International Conference on Site Characterization, Taipei, Taiwan, CD, 6.
31. Ladd CC, DeGroot DJ (2003) Recommended practice for soft ground site characterization: Arthur Casagrande Lecture. Proceedings 12th Panamerican Conference on Soil Mechanics and Geotechnical Engineering, Boston, MA, 3–57.
32. Robertson PK (2009) Interpretation of cone penetration tests—a unified approach. *Can Geotech J* 46: 1337–1355.
33. Robertson PK (1990) Soil classification using the cone penetration test. *Can Geotech J* 27: 151–158.
34. Robertson PK, Campanella RG, Gillespie D, et al. (1986) Seismic CPT to measure in situ shear wave velocity. *J Geotech Eng* 112: 791–803.
35. Campanella RG, Stewart WP (1992) Seismic cone analysis using digital signal processing for dynamic site characterization. *Can Geotech J* 29: 477–486.
36. Landon MM, DeGroot DJ (2006) Measurement of small strain shear modulus anisotropy on unconfined clay samples using bender elements. *Proceedings GeoCongress '06: Geotechnical Engineering in the Information Technology Age*, ASCE Geo-Institute, CD, 6.
37. Jamiolkowski R, Lancellotta R, Lo Presti DCF (1995) Remarks on the stiffness at small strains of six Italian clays. *Developments in Deep Foundations and Ground Improvement Schemes: Symp on Geotextiles, Geomembranes and Other Geosynthetics in Ground Improvement*, 197–216.
38. Pennington DS, Nash DFT, Lings ML (1997) Anisotropy of G_0 shear stiffness in Gault clay. *Géotechnique* 47: 391–398.
39. DeGroot DJ, Landon MM, Ryan RM (2007) Objective evaluation of preconsolidation stress for soft clays from constant rate of strain pore pressure data. *Adv Meas Model Soil Behav*.
40. Lunne T, Berre T, Andersen KH, et al. (2006) Effects of sample disturbance and consolidation procedures on measured shear strength of soft marine Norwegian clays. *Can Geotech J* 43: 726–750.
41. Terzaghi K, Peck RB, Mesri G (1996) *Soil Mechanics in Engineering Practice*. John Wiley and Sons, New York, 549.
42. Becker DE, Crooks JH, Been K, et al. (1987) Work as a criterion for determining in situ and yield stresses in clays. *Can Geotech J* 24: 549–564.
43. Mesri G, Feng TW (1992) Constant rate of strain consolidation testing of soft clays. *Proceedings Marsal Symp*, Mexico City, 49–59.
44. Mesri G, Lo DOK, Feng TW (1994) Settlement of embankments on soft clays. Proceedings of ASCE conference on vertical and horizontal deformations of foundations and embankments, College Station, Texas, 1: 8–56.
45. Leroueil S (1996) Compressibility of clays: fundamental and practical aspects. *J Geotech Eng* 122: 534–543.

46. Jamiolkowski M, Ladd CC, Germaine JT, et al. (1985) New developments in field and laboratory testing of soils. Proceedings 11th International Conference on Soil Mechanics and Foundation Eng, San Francisco, 1: 57–154.
47. Lunne T, Robertson PK, Powell JJM (1997) *Cone Penetration Testing In Geotechnical Practice*. Spoon Press, London.
48. Mayne PW (2007) *Cone Penetration Testing: A Synthesis of Highway Practice*. NCHRP Synthesis 368. Transportation Research Board, Washington, D.C.
49. Menzies BK (1988) A computer controlled hydraulic triaxial testing system. Donaghe RT, Chaney RC, Silver ML, Eds., *Advanced Triaxial Testing of Soil and Rock*, ASTM STP 977, American Society for Testing and Materials, Philadelphia, 82–94.
50. Wissa AEZ, Christian JT, Davis EH, et al. (1971) Consolidation at constant rate of strain. *J Soil Mech Found Div* 97: 1393–1413.
51. Mesri G, Hayat TM (1993) The coefficient of earth pressure at rest. *Can Geotech J* 30: 647–666.
52. Sandbækken G, Berre T, Lacasse S (1986) Oedometer testing at the Norwegian Geotechnical Institute. *Consolidation of Soils: Testing and Evaluation*, ASTM STP 892: 329–353
53. Tavenas R, Jean P, Leblond P, et al. (1983) The permeability of natural soft clays, Part II: permeability characteristics. *Can Geotech J* 20: 645–660.
54. Baligh MM, Levadoux JN (1986) Consolidation after undrained piezocone penetration, II Interpretation. *J Geotech Eng* 112: 727–745.
55. Germaine JT, Ladd CC (1988) State-of-the-Art: Triaxial testing of saturated cohesive soils. *Advanced Triaxial Testing of Soil and Rock*, ASTM STP 977: 421–459.
56. Lacasse S, Berre T (1988) State-of-the-Art: Triaxial testing methods for soils. *Advanced Triaxial Testing of Soil and Rock*, ASTM STP 977: 264–289.
57. Bjerrum L (1973) Problems of soil mechanics and construction on soft clays. *Proceedings 8th International Conference Soil Mech and Found Eng*, Moscow, 3: 111–159.
58. Bjerrum L, Landva A (1966) Direct simple shear tests on Norwegian quick clay. *Géotechnique* 16: 1–20.
59. DeGroot DJ, Ladd CC, Germaine JT (1992) *Direct Simple Shear Testing of Cohesive Soils*, Research Report No. R92-18, Center for Scientific Excellence in Offshore Engineering, MIT, Cambridge, MA.
60. Ladd CC (1991) Stability evaluation during staged construction (22nd Terzaghi Lecture). *J Geotech Eng* 117: 540–615.
61. Mesri G (2001) Undrained shear strength of soft clays from push cone penetration test. *Géotechnique* 51: 167–168.
62. Baligh MM, Azzouz AS, Chin CT (1987) Disturbances due to ideal tube sampling. *J Geotech Eng* 113: 739–757.
63. Clayton CRI, Siddique A, Hopper RJ (1998) Effects of sampler design on tube sampling disturbance—numerical and analytical investigations. *Géotechnique* 48: 847–867.
64. Hight DW (2003) Sampling effects in soft clay: An update on Ladd and Lambe (1963). *Soil Behav Soft Ground Constr*, 86–122.
65. DeGroot DJ (2003) Laboratory measurement and interpretation of soft clay mechanical behavior. *Soil Behav Soft Ground Constr*, 167–200.
66. Tanaka H, Sharma P, Tsuchida T, et al. (1996) Comparative study on sample quality using several types of samplers. *Soils Found* 36: 57–68.

67. Hight DW, McMillan F, Powell JJM, et al. (2003) Some Characteristics of London Clay. Proceedings of the International Workshop on Characterisation and Engineering Properties of Natural Soils, Singapore, 2: 851–907.
68. Donohue S, Long M (2010) Assessment of sample quality in soft clay using shear wave velocity and suction measurements. *Géotechnique* 60: 883–889.
69. Berman DR, Germaine JT, Ladd CC (1993) Characterization of engineering properties of Boston blue clay for the MIT campus. *Research Rep. 93-16*, Dept of Civil and Environmental Engineering, Massachusetts Institute of Technology, Cambridge, MA.
70. Ladd CC, Whittle AJ, Legaspi DE (1994) Stress-deformation behavior of an Embankment on Boston Blue Clay. Proceedings of ASCE conference on vertical and horizontal deformations of foundations and embankments, College Station, Texas, 2: 1739–1759.
71. Ladd CC, Young GA, Kraemer SR, et al. (1999) Engineering properties of Boston blue clay from special testing program. Proceedings Special Geotechnical Testing: Central Artery/Tunnel Project in Boston, Massachusetts, ASCE, Reston, VA, 1–24.
72. Koutsoftas DC, Ladd CC (1985) Design strengths for an offshore clay. *J Geotech Eng* 111: 337–355.
73. Kulhawy FH, Mayne PW (1990) *Manual on Estimating Soil Properties for Foundation Design*, Report No. EL-6800, EPRI, Palo Alto, CA, 306.
74. Mitchell TJ, DeGroot DJ, Lutenecker AJ, et al. (1999) Comparison of CPTU and laboratory soil parameters for bridge foundation design on fine grained soils: A case study in Massachusetts. *Transp Res Rec* 1675: 24–31.
75. Vaghar S, Bobrow DJ (1998) Comparison of two excavation support systems in clay: Central Artery Tunnel, Boston, Massachusetts, USA. 4th International Conference on Case Histories in Geotechnical Engineering, St. Louis, Missouri.
76. Hashash YMA, Whittle AJ (1996) Ground movement prediction for deep excavations in soft clay. *J Geotech Eng* 122: 474–486.
77. Orazalin ZY, Whittle AJ, Olsen MB (2015) Three-dimensional analyses of excavation support system for the Stata Center basement on the MIT campus. *J Geotech Geoenvironmental Eng* 141: 05015001.
78. Whittle AJ, Hashash YMA, Whitman RV (1993) Analysis of deep excavation in Boston. *J Geotech Eng* 119: 69–90.
79. Whittle AJ, Corral G, Jen LC, et al. (2015) Prediction and Performance of Deep Excavations for Courthouse Station, Boston. *J Geotech Geoenvironmental Eng* 141: 04014123.
80. Hagerty D, Peck R (1971) Heave and Lateral Movements due to Pile Driving. *J Soil Mech Found Div* 97: 1513–1531.
81. Dugan Jr JP, Freed DL (1984) Ground Heave Due to Pile Driving. 1st International Conference on Case Histories in Geotechnical Engineering, St. Louis, Missouri.
82. Abedi H, Risitano J, Yamane D, et al. (1993) Performance of Wick Drains in Bon Blue Clay. 3rd International Conference on Casoste Histories in Geotechnical Engineering, St. Louis, Missouri.



AIMS Press

© 2019 the Author(s), licensee AIMS Press. This is an open access article distributed under the terms of the Creative Commons Attribution License (<http://creativecommons.org/licenses/by/4.0>)